Eskil Reitan Kvamvold

Functional characterization of the antennal-lobe glomeruli constituting the macro glomerular complex and the posterior complex in the moth brain

Master's thesis in Neuroscience

Trondheim, June 2019

Supervisor: Elena Ian
Co-supervisor: Bente G. Berg

Norwegian University of Science and Technology
Faculty of Medicine and Health Sciences
Kavli Institute for Systems Neuroscience

NTNU
Norwegian University of
Science and Technology

Abstract

In order to understand how information is processed in a neural circuit, it is important to have an in-depth overview of all aspects of the circuit. For exploring the coding principles of the antennal lobe (AL), it is necessary to clarify the function of the glomeruli since they constitute the synaptic regions between the first- and second-order neurons in the olfactory circuit. The aim of the present study was to functionally characterize the AL output neurons confined to the medial antennal lobe tract (ALT) originating from two distinct groups of glomeruli in the AL, i.e. the macro glomerular complex (MGC) and the posterior complex (PCx). This was done through retrograde staining of the uniglomerular medial ALT neurons, providing the possibility to record from the dendrites of these neurons in the AL using calcium imaging. The present study demonstrates the first attempt to investigate the MGC and the PCx activity in a heliothine moth in response to a set of pheromones and interspecific components using this method. The application of these odor stimuli onto the antenna of the living moth evoked odor-specific responses in the labelled PNs, visualized as distinct activation maps of glomeruli in the MGC and PCx. The present thesis shows that the three MGC glomeruli mainly had responses to the following stimuli: in the Cumulus to the primary pheromone component, Z11-16:ald; in the DMA to the two interspecific components Z9-14:ald and Z11-16:OH; and in the DMP to the secondary pheromone Z9-16:ald and the interspecific component Z9-14:ald. The PCx glomeruli responded to four minor pheromones, i.e. 7:ald, 9:ald, 14:ald, and Z7-16:ald. In addition to component blends constituting the interspecific substances, and the primary- and secondary pheromones.

Acknowledgements

The experimental work presented in this master's thesis have been conducted in the Chemosensory laboratory at the Department of Psychology, Norwegian University of Technology and Science.

A special thanks goes out to my main supervisor Elena Ian for teaching me all the experimental procedures, how to interoperate the data and in general spending her valuable time helping me out. Also, I would like to thank my co-supervisor and leader of the Chemosensory lab Bente G. Berg for her valuable input on the project and her time spent helping to structure this thesis. Thanks to Xi Chu for helping me clean my data, and for her input on statistical analysis. I would also like to express my gratitude to all my fellow lab members for providing me with interesting conversations, great experiences, and support during my time spent at the lab. Finally, I would like to thank my partner, Marthe Victoria, for all her love and support.

Table of contents

Abstract iii
Acknowledgements v
Abbreviations ix

1 Introduction 1

1.1 Olfactory processing 1

1.1.1 Pheromones and interspecific components 1
1.1.2 Odor detection in the periphery 2
1.1.3 Antennal lobe 3

1.1.3.1 Neural elements of the antennal lobe 4
1.1.3.2 Glomerular organization of the AL 6

1.1.3.2.1 Macro Glomerular Complex 6
1.1.3.2.2 Posterior Complex 7
1.1.3.2.3 Ordinary Glomeruli 9

1.1.4 Higher bran areas 10

1.2 Calcium imaging 11
1.3 Aims 12

2 Materials and methods 13

2.1 The insects 13
2.2 Insect preparation 13
2.3 Odor stimulation 14
2.4 Imaging 16
2.5 Data processing and Statistical analysis 16
2.6 Data Cleaning 18
2.7 Ethics 20

3 Results 21

3.1 MGC glomeruli responses 22

3.1.1 Odor-evoked responses in the Cumulus 22
3.1.2 Odor-evoked responses in the small MGC-unit located anteriorly, DMA 24
3.1.3 Odor-evoked responses in the small MGC-unit located posteriorly, DMP 27

3.3 Odor-evoked responses in the posterior complex, PCx 30
3.4 Comparison of odor-evoked responses to different stimulus concentrations 34

4 Discussion 37

4.1 Functional characterization of the macro-glomerular complex 37

4.1.1 Odor-evoked responses in the cumulus 37
4.1.2 Odor-evoked responses in the DMA 38
4.1.3 Odor evoked responses in the DMP 39

4.2 Functional characterization of the posterior complex 40
4.3 The effect of stimulating with different concentrations 41
4.4 The role of the minor pheromone components 43
4.5 Methodical considerations 44

4.5.1 Calcium imaging 44
4.5.2 Analysis 45

4.6 Further investigation 46

5 Conclusion 49

References .....
Appendix A .....

Abbreviations

AL	Antennal lobe
ALT	Antennal lobe tract
DMA	Dorso-medial anterior
DMP	Dorso-medial posterior
LN	Local interneuron
LPOG	Labial-palp pit organ glomeruli
MGC	Macro glomerular complex
OR	Odor receptor
OSN	Olfactory sensory neuron
PCx	Posterior complex
PN	Projection neuron
ROI	Region of interest

1 Introduction

For a wide variety of organisms, the sense of smell is vital for survival. Many vertebrates and invertebrates rely on the information obtained through the olfactory system for finding food, shelter, and mate, while avoiding predators. (Doty, 1986; Hansson, 1999). The olfactory system is evolutionary well preserved throughout the animalia, and remarkable anatomical and functional similarities can be found in both vertebrates and invertebrates, spanning everything from odorant receptor proteins to odor guided behavior and memory (Reviewed: Ache & Young, 2005; Hildebrand & Shepherd, 1997; Kaupp, 2010). Therefore, comparative discoveries across animal species is interesting on both cellular and molecular mechanisms (Mizunami, Yokohari, & Takahata, 2004).

In the relatively simple olfactory system of the insects, the sensory input is only a few neural layers away from the behavioral output, and thus, provides a simplified arrangement for investigating the system as a whole. The last, combined with the fact that insects have an easily accessible nervous system, and a highly advanced sense of smell, makes them an attractive model for studying olfaction (Reviewed: Martin et al., 2011). Among the insects most frequently used for exploring coding principles underlying olfaction, are noctuid moths. The Heliothinae moths, a monophyletic subfamily distributed on all continents have been extensively studied over the last decades, also because these organisms include some of the most serious worldwide pests. Heliothinae males possess an incredible sensitivity and consistent behavioral response to female-produced compounds, including pheromones produced by females of the same species as well as components of heterospecific sympatric females. Therefore, the male *Helicoverpa armigera* is used as a model organism for this project.

1.1 Olfactory processing

1.1.1 Pheromones and interspecific components

The term pheromone was first defined by Karlson and Luscher (1959), and states the following: *'' ...substance which are secreted to the outside by an individual and received by a second individual of the same species, in which they release a specific reaction…''* (s.55). Heliothinae moths use a multicomponent pheromone blends for sexual attraction; these pheromone blends are slightly different for each specific species, which help them find a suitable mate (Hillier & Baker, 2016). Each species' blend usually consists of two behaviorally relevant pheromone

components, one primary and one secondary (Reviewed: Berg, Zhao, & Wang, 2014). In addition to these two components, the female emits several other chemicals, usually called minor pheromone components. The role of the minor components is not fully understood, however. Interestingly, within closely related species living in the same geographical area (sympatric species), one component acting as a pheromone, inducing attraction in one species, might act as a behavioral antagonist in a sympatric species. A female-produced component suppressing attraction from a heterospecific male is therefore referred to as an interspecific component.

For the moth studied here, *H. armigera*, four main components have been shown to affect the sexual behavior, two pheromone components and two behavioral antagonists: the primary pheromone component, *cis*-11-hexadecenal (Z11-16:ald), the secondary pheromone component, *cis*-9-hexadecenal (Z9-16:ald), and the two interspecific components, *cis*-9-tetradecenal (Z9-14:ald) and *cis*-11-hexadecenol (Z11-16:OH) (Reviewed: Berg et al., 2014). Newer findings, however, have also reported that *cis*-11-hexadecenyl acetate (Z11-16:ac) acts as an interspecific component (Xu et al., 2016). Although the component Z9-14:ald is defined as an interspecific component, smaller amounts of this component in a blend with the primary and the secondary component have shown to increase attraction of *H. armigera* (Wu et al., 2015; Zhang, Salcedo, Fang, Zhang, & Zhang, 2012). Additionally, a study by Zhang et al. (2012), has identified electrophysiological responses in the antennae of a male *H. armigera* to ten different components that were extracted from the female sex gland, indicating that several components than those described above might be involved in sexual attraction.

1.1.2 Odor detection in the periphery

The first step in creating a sense of smell is the detection of odorants in the environment. The moth detects volatile airborn molecules via olfactory sensory neurons housed inside small hair-like structures named sensilla, which are mainly located on their antennae (Keil, 1999; Stengl, Ziegelberger, Beoekhoff, & Krieger, 1999). The pores on the outer segment of the sensilla allow for the passage of molecules to enter the sensillum lymph (Reviewd: Steinbrecht, 1997). This sensillar lymph are reported to have a high concentration of odor-binding proteins (Vosshall, 2000). Although not confirmed, these proteins have been assumed to be involved in transporting the molecules to the olfactory receptors (OR) located at the dendrites of bipolar olfactory sensory neurons (OSN) within the sensilla. On the other hand, a study by Laughlin et al. (2008) has suggested that the pheromone-binding proteins are involved in activation of

specific ORs, via a pheromone-induced conformational shift in these proteins. The moth pheromone activated OSNs are located inside male specific sensilla trichodea, which are usually composed of two to three OSNs in each sensillum (Baker et al., 2004; Berg, Almaas, Bjaalie, & Mustaparta, 2005; Cossé, Todd, & Baker, 1998). So far, three different categories of trichodea sensillum have been suggested in the *H. armigera*: sensillum A, B, and C. Sensillum B can be further divided into two sub-types, while sensillum C can be divided into three sub-types (Xu et al., 2016). The tuning profile of an OSN is dependent on how many receptor types each single OSN expresses, and how many odorants that activates the specific OR. In the fruit fly, *Drosophila melanogaster*, the general pattern is that one OSN expresses only one receptor type (Vosshall, 2000); however, there have been reported instances where several OR types are expressed per OSN (Goldman, Van der Goes van Naters, Lessing, Warr, & Carlson, 2005). The same organization can be assumed in the moth as well, as several electrophysiological studies have shown that several OSNs excited by pheromone components seem to be narrowly tuned to one specific pheromone (Jiang et al., 2014; Liu, Liu, Lin, & Wang, 2013; Xu et al., 2016; Xu, Papanicolaou, Liu, Dong, & Anderson, 2015); whereas other OSN are excited by several pheromone components (Jiang et al., 2014; Xu et al., 2016).

1.1.3 Antennal lobe

The axons of the OSNs make up the antennal nerve, which projects directly into the antennal lobe (AL). The AL is the primary olfactory center of the moth brain and is easily distinguishable as a sphere anterior to the protocerebrum, clearly demarcated from the rest of the brain. The anatomical organization of the primary olfactory center is well retained throughout the animalia, and the AL can be seen as homologous to the vertebrate's olfactory bulb. These structures are easily recognizable due to their spheroidal neuropil compartments, glomeruli (Anton & Homberg, 1999), which are separated from each other by glia cells (Tolbert & Hildebrand, 1981). The glomeruli cover mainly the outer part of the AL, enclosing a glomerulus-free core (Zhao, Chen, et al., 2016). The AL receives sensory information primarily from the antennal OSNs. However, there is a subset of OSNs located in the labial-palp pit organ, which conveys information about CO_2 to one large glomerulus located ventrally in the AL, the labial palp pit organ glomerulus (LPOG) (Kent, Harrow, Quartararo, & Hildebrand, 1986; Zhao et al., 2013). The antennal OSNs enter the ipsilateral AL through the dorsolateral part of the lobe. In Drosophila, all OSNs expressing a given OR gene are shown to project to one or two glomeruli in the AL, creating an odotopic map in the AL (Clyne et al.,

1999; Couto, Alenius, & Dickson, 2005; Gao, Yuan, & Chess, 2000; Vassar et al., 1994; Vosshall, 2000; Vosshall, Amrein, Morozov, Rzhetsky, & Axel, 1999). This kind of organization has been supported in Heliothinae moths as well, via electrophysiological studies combined with tracing experiments (Berg, Almaas, Bjaalie, & Mustaparta, 1998; Berg et al., 2005; Hansson, Almaas, & Anton, 1995; Lee, Baker, & Vickers, 2006; Lee, Carlsson, Hansson, Todd, & Baker, 2006).

1.1.3.1 Neural elements of the antennal lobe

In addition to the OSN input, the AL embodies three additional neuronal types: projection neurons (PN), local interneurons (LN), and centrifugal neurons (Anton & Homberg, 1999). The PNs and LNs have their somata located in three distinct cell clusters surrounding the AL: the lateral- , medal- , and anterior cell cluster (Anton & Homberg, 1999; Homberg, Christensen, & Hildebrand, 1989; Malun, Waldow, Kraus, & Boeckh, 1993; Rybak et al., 2016; Sun, Tolbert, & Hildebrand, 1997). The medial and anterior cell clusters consist of somata of PNs exclusively, while the lateral cell cluster includes somata of all LN as well as some PNs (Homberg, Montague, & Hildebrand, 1988).

The PNs convey olfactory information to the higher brain areas; predominantly to the lateral protocerebrum and the calyces of the mushroom body. The PNs connect to these higher brain areas through a total of six parallel AL tracts (ALT) (Figure 1) (Homberg et al., 1988; Ian, Berg, Lillevoll, & Berg, 2016; Ian, Zhao, Lande, & Berg, 2016; Rø, Muller, & Mustaparta, 2007). Three of which is referred to as the main ALTs: the medial ALT, medio-lateral ALT, and the lateral ALT. In addition to three smaller ALTs: the transverse ALT, the dorsomedial ALT, and the dorsal ALT. For this project however, the medial ALT is of interest, as it creates the main connection between the AL and the calyces (Ian, Berg, et al., 2016). This connection allows for staining of these PNs in the calyces, while recording the activity of the very same PNs on a glomerular level through calcium imaging. This process however, will be explained in greater detail at a later point. After exiting the AL, the medial ALT projects posteriorly, ventrally of the edge of the central body, before turning laterally at the posterior end of the protocerebrum. Here it passes anteriorly of the calyces and send terminal branches into this cup-shaped structure before terminating in one or several areas in the lateral protocerebrum (Figure 1). The medial ALT consists of approximately 400 axons in *M. sexta* (Homberg et al., 1988), and a large majority of these are uniglomerular, meaning that they originate in one glomerulus only (Berg et al., 2014). However, several other neuron types are classified in this

tract as well; these include both uniglomerular and multiglomerular PNs where some innervate the calyces while others don't, before they terminate in different areas throughout the lateral protocerebrum (Ian, Zhao, et al., 2016).

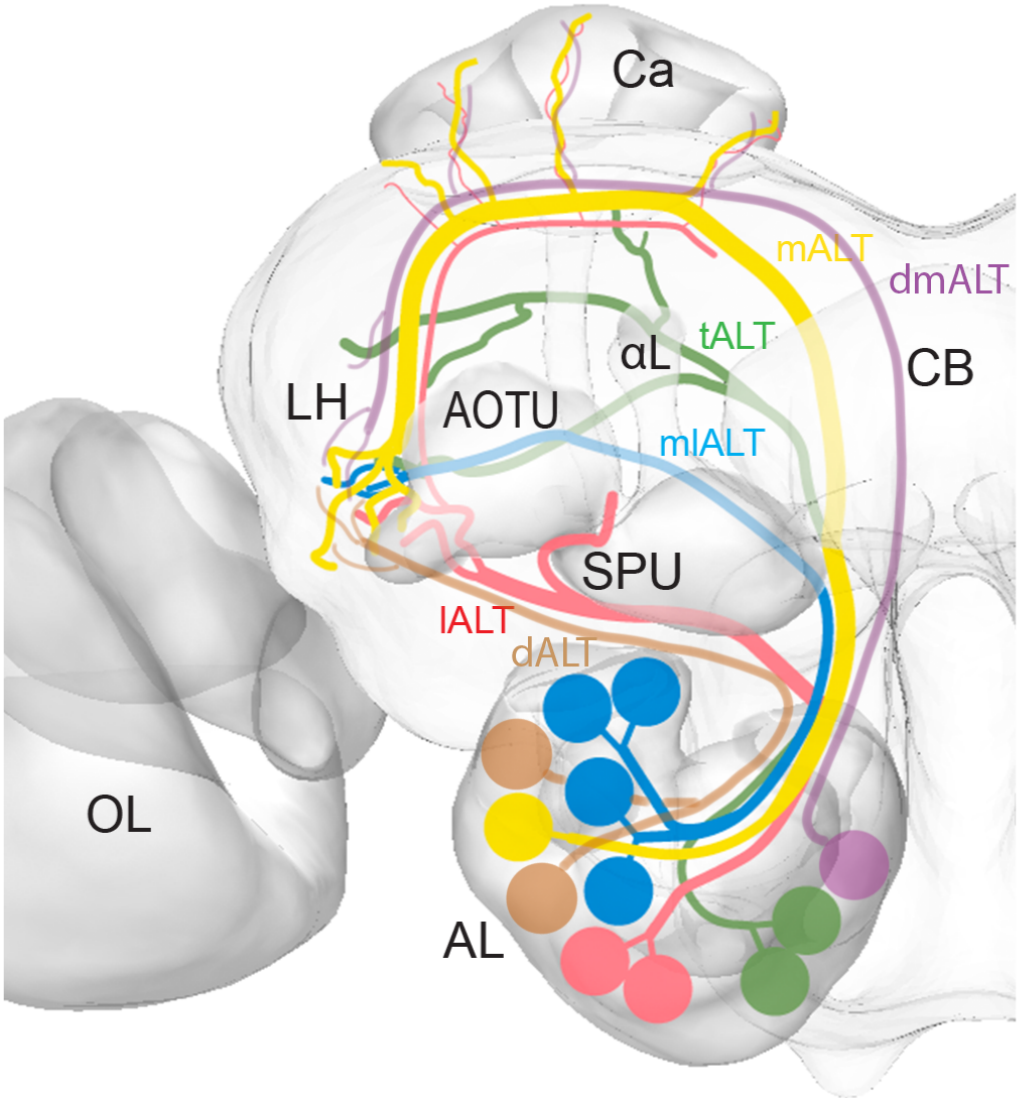

Figure 1. Schematic overview of the antennal-lobe tract (ALTs) in the moth brain from a dorsal view. Tracts with mainly uniglomerular projection neurons (PN) are represented with only one glomerulus in the antennal lobe (AL), while tracts mainly consisting of multiglomerular PNs are represented with four glomeruli in the AL, while two glomeruli in the AL represents tracs that have a mix of both uniglomerular and multiglomerular PNs. The yellow color represents the medial ALT, the blue the medio-lateral ALT, the red the lateral ALT, the green the transvers ALT, the purple the dorso-medial ALT, and the orange the dorsal ALT. OL, optic lobe; SPU, spur of the mushroom body; CB, central body; AOTU, anterior optic tubercle; LH, lateral horn; αL, alpha lobe; Ca, calyces. Modified from (Ian, Berg, et al., 2016).

The LNs operating exclusively within the AL have a fundamental role in determining the properties of the signals that are carried to the higher brain areas. The LNs can shape the signals within the AL in two main ways: 1) by synchronizing activity across glomeruli (Lei, Christensen, & Hildebrand, 2002, 2004), and 2) by providing the system with lateral inhibition (Martin et al., 2011). Like in other insects, most LN in moths are GABAergic (Berg,

Schachtner, & Homberg, 2009; Hoskins, Homberg, Kingan, Christensen, & Hildebrand, 1986; Lei et al., 2002); however, Berg et al. (2009) have reported a few non-GABAergic LNs in the heliothine moth. A population of excitatory cholinergic LNs has actually been reported in Drosophila (Chou et al., 2010; Shang, Claridge-Chang, Sjulson, Pypaert, & Miesenböck, 2007).

The centrifugal neurons make up the smallest group of AL neurons and are assumed to play a modulatory role. These neurons have their somata and dendritic branches located outside the AL, while having axonal projections into the AL (Anton & Homberg, 1999; Schachtner, Schmidt, & Homberg, 2005). Several different types of the centrifugal neurons have been identified, including both serotonergic (Dacks, Christensen, & Hildebrand, 2006) and octopaminergic types (Dacks, Christensen, Agricola, Wollweber, & Hildebrand, 2005).

1.1.3.2 Glomerular organization of the AL

The AL of *H. armigera* is sexually dimorphic; this is mainly due to the male specific macro glomerular complex (MGC) (Skiri, Rø, Berg, & Mustaparta, 2005; Zhao, Chen, et al., 2016; Zhao, Ma, et al., 2016). The male AL consists of an average of 79 glomeruli, which can be divided into four categories: the ordinary glomeruli, MGC, posterior complex (PCx), and the LPOG (Zhao, Chen, et al., 2016). As described earlier the LPOG category consists of one large glomerulus conveying information about CO_2. The remaining three categories are explained below; the MGC and the PCx in greater detail as they are of interest in this project.

1.1.3.2.1 Macro Glomerular Complex

The anatomical organization of the AL of the male moth is quite specific due to the sexually dimorphic MGC comprising the unit of male-specific glomeruli. This area is responsible for processing input about the female produced pheromones. The MGC of *H. armigera* comprises three glomeruli, of which the largest is named cumulus, and is situated at the base of the antennal nerve. The other two glomeruli are named according to their position relative to the cumulus: dorsomedial-anterior (DMA) and dorsomedial-posterior (DMP) (Figure 2) (Skiri et al., 2005; Zhao, Chen, et al., 2016). Based on current knowledge, the cumulus receives information exclusively from OSNs exited by the primary pheromone (Z11-16:ald), the DMA receives information mainly from the two well-known interspecific components (Z9-14:ald and Z11-16:OH), however, to a lesser degree, also receives input from OSNs responding to a third

interspecific component Z11-16:ac. The DMP receives input from OSNs responding to the secondary pheromone component (Z9-16:ald), and one of the interspecific component (Z9-14:ald) (Figure 3) (Xu et al., 2016). Previous studies on MGC PNs in heliothine moths have demonstrated that they project through several ALTs, but most of these reports have focused on uniglomerular PNs passing in the medial ALT, which seem to be relatively narrowly tuned (rewived: Berg et al., 2014). However, instances of synergistic response patterns to species-specific pheromone blends have also been reported in these uniglomerular PNs (Berg et al., 1998; Vickers, Christensen, & Hildebrand, 1998).

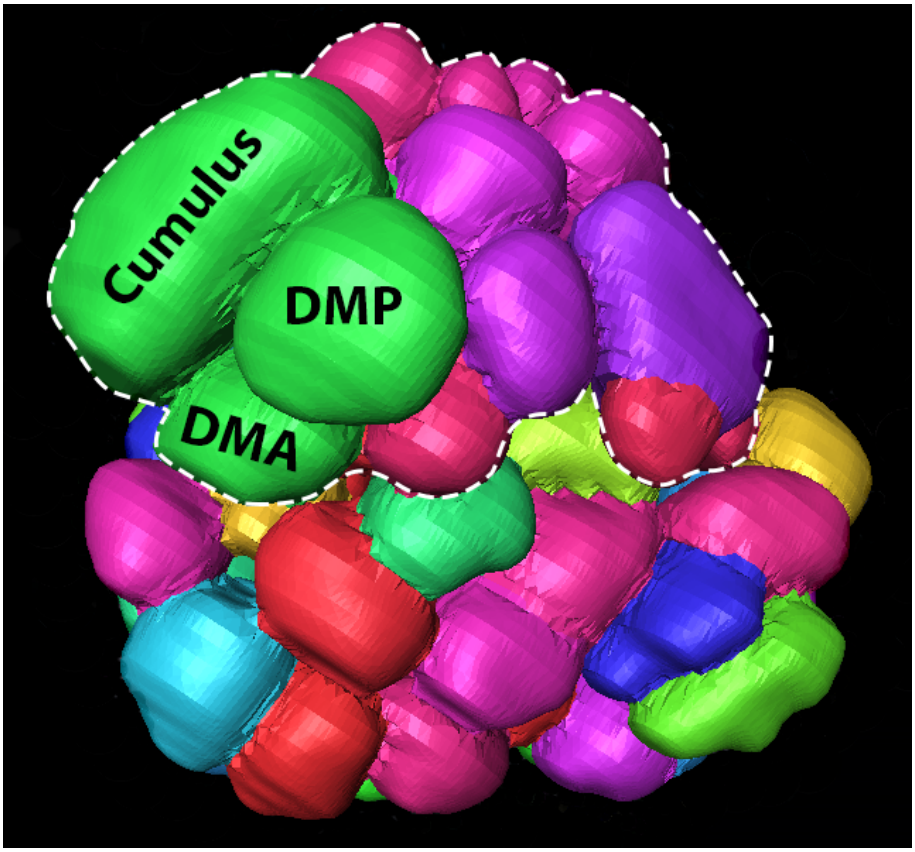

Figure 2. AMIRA model of the male AL from a dorsal view. The stippled white line outlines the macro glomerular complex (MGC) and the posterior complex (PCx). The green glomeruli inside the white stippled line represents the MGC, while the different shades of purple inside the line represents the PCx. Glomeruli outside the white stippled line are ordinary glomeruli. DMA, dorsomedial-anterior; DMP, dorsomedial-posterior.

1.1.3.2.2 Posterior Complex

The PCx is located posterior and ventral to the MGC, close to the medial cell cluster and the anterior wall of the protocerebrum. This means that not all PCx glomeruli can be easily seen during imaging, however greatest chance is given with a dorsal view of the AL as represented

in Figure 2. However, this orientation does not account for the medial cell cluster and the protocerebrum that might block the view. Although the AL differences between sexes are most distinct in the sex-specific glomeruli (MGC), one can also see noteworthy differences in the PCx between males and females. Whereas the PCx of the male consists of ten glomeruli, the female has only nine.

Moreover, the average glomerular volume in the PCx is higher in males as compared to females (Zhao, Chen, et al., 2016; Zhao, Ma, et al., 2016). These differences could indicate that its relevance differs between the sexes. The detailed anatomical mapping of the male *H. armigera* AL provided new evidence regarding the glomeruli located in the PCx (Zhao, Chen, et al., 2016). This study shows that the PCx glomeruli are clearly separated from the ordinary glomeruli; additionally, in the *Drosophila* it is also found that the OSNs that possess genetically similar OR project to adjacently located glomeruli in the AL (Couto et al., 2005). Based on this information, one could hypothesize that the PCx either could be involved in pheromone processing as it is located close to the MGC glomeruli, or at least has a function distinct from the ordinary glomeruli, as these two groups are clearly demarcated from each other. Furthermore, for several of the heliothine species studied, including *Helicoverpa zea, Heliothis virescens, Helicoverpa assulta*, and *Heliothis subflexa*, the sensory neuron co-located with the neuron tuned to Z11-16:ald has been found to project to one of the PCx glomerulus located close to the MGC (Figure 3) (Berg et al., 1998, 2005; Lee, Baker, et al., 2006; Lee, Carlsson, et al., 2006; S. G. Lee, Poole, Linn, & Vickers, 2016). Additionally, the type B sensillum in *H. subflexa* and *H. virescens* has also been reported to have a sensory axon ending up in a PCx glomerulus, located nearby the MGC (Figure 3). These axons originate from neurons that are co-located with a neuron tuned to Z9-16:ald/Z9-14:ald (Lee, Baker, et al., 2006; Lee et al., 2016). It should be noted that the two types of co-located neurons mentioned here, target two separate glomeruli in the PCx. These facts might indicate that a part of the PCx could be involved in pheromone processing. However, a functional characterization of the type A sensillum (tuned to Z11-16:ald) in *H. armigera* by Xu et al. (2016) found responses only to the primary pheromone, leaving both the ligand and the function of the of the co-located neurons projecting to the PCx unknown. So far, the PCx glomeruli have been reported to be innervated by PNs in the medial ALT having their somata located in the medial cell cluster (Zhao, Chen, et al., 2016). Nevertheless, the function of any of the PCx glomeruli is still unclear.

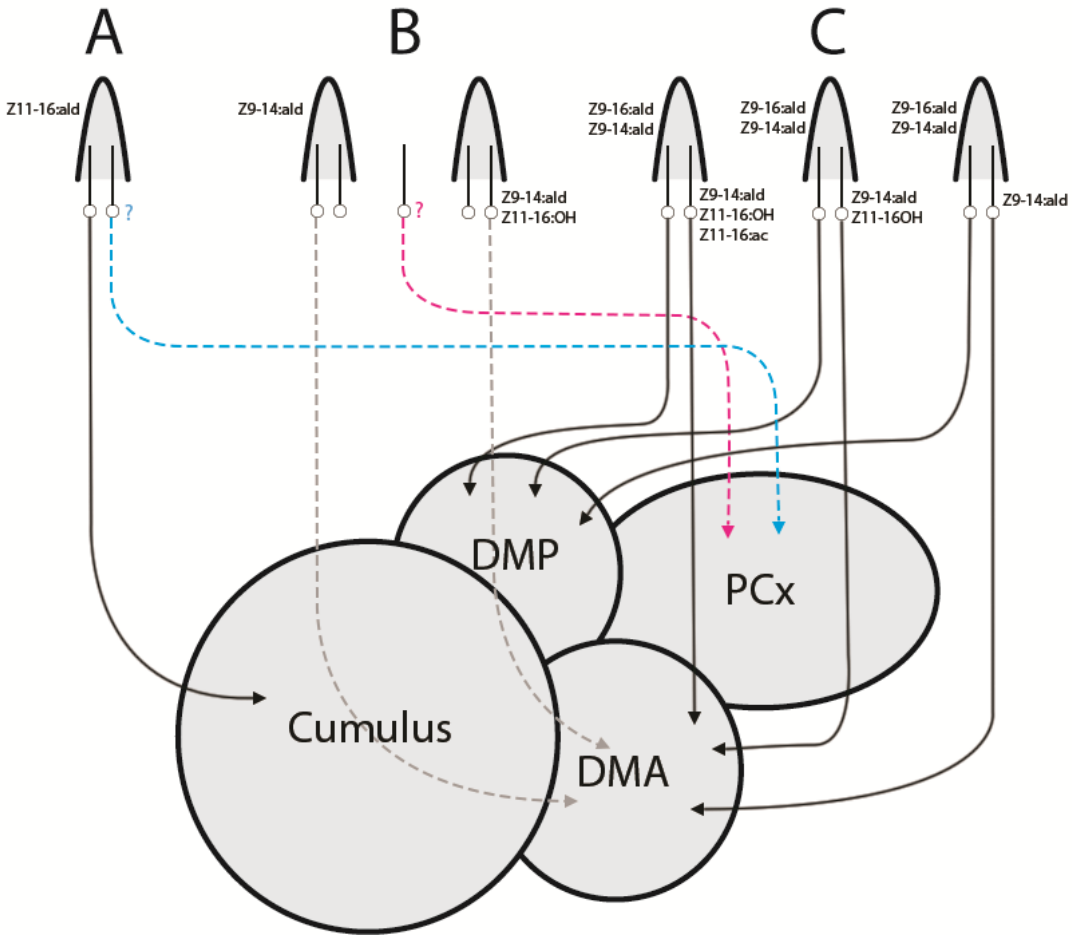

Figure 3. Model of the peripheral coding of pheromones in the antennae and the projections of male-specific sensory neurons into the AL. The solid black line, and the gray stippled line is based on data from Wu et al. (2015) and Xu et al. (2016). The dotted grey line is not confirmed; however, it has been suggested by Xu et al. (2016). While the dotted blue is not confirmed in the H. armigera, it is mapped both in Helicoverpa zea, Helicoverpa assulta, Heliothis Virescens, and Heliothis subflexa (Berg et al., 1998, 2005; Lee, Baker, et al., 2006; Lee, Carlsson, et al., 2006). The pink line has not been shown in the H armigera, however, one of the neurons confined to a type B sensillum in H. subflexa and H. virescens is found to project to the PCx (Lee, Baker, et al., 2006; Lee et al., 2016). Although the pink and blue line target the same PCx unit in this model, it should be noted that in reality, the two types of sensory neurons project to two independent PCx glomeruli. A question mark next to a neuron means that its ligand is unknown.

1.1.3.2.3 Ordinary Glomeruli

The ordinary glomeruli refer to all glomeruli that is not confined to the MGC, PCx or the LPOG. This group consist of a total of 64-65 glomeruli in the male *H. armigera*, and 66 in the female, making it by far the largest group of AL glomeruli. The main task of these glomeruli is processing of information about general odors; however, they might also be involved in detection of input from thermal (humidity and temperature) and mechanical stimuli

(Guerenstein, Christensen, & Hildebrand, 2004; Han, Hansson, & Anton, 2005). All glomeruli outside the white stippled line in Figure 2 represent ordinary glomeruli.

1.1.4 Higher bran areas

As mentioned above, the two main targets of the ALTs are the calyces of the mushroom body and the lateral protocerebrum. The mushroom body consist of Kenyon cells, which are intrinsic neurons (Laurent & Naraghi, 1994) that apply a sparse coding strategy (Jortner, Farivar, & Laurent, 2007). The calyces are the input areas to the mushroom body lobes. And as seen in Figure 1, the calyces have no or minimal connections to several of the ALTs. And as previously mentioned, the medial ALT is responsible for the main olfactory input from the AL. Although, some smaller amount of innervation can also be seen from the dorsomedial-, transverse-, and the lateral ALTs. However, the calyces are not a terminal point for olfactory information exclusively, as it incorporates gustatory, visual, and mechanosensory information as well, making it a multisensory integration unit (Stopfer, 2014). The mushroom body has been shown to be important for establishment of odor memory (reviewed: Stopfer, 2014). This is based on studies in a variety of insects showing that: increased volume of the mushroom bodies with increased experience (Maleszka, Barron, Helliwell, & Maleszka, 2009), retrograde amnesia by cooling of the calyces after olfactory training (Menzel, Erber, & Masuhr, 1974), and the fact that insects have visual and olfactory learning deficits, caused by abnormalities in the mushroom bodies (de Belle & Heisenberg, 1994; Heisenberg, Borst, Wagner, & Byers, 1985; Liu, Wolf, Ernst, & Heisenberg, 1999; McBride et al., 1999).

The lateral protocerebrum does not refer to a specific neuropil, but instead consists of a range of neural areas (Ito et al., 2014) as the lateral horn, the inferior neuropil, the anteroventral lateral protocerebrum, the superior neuropil, the ventromedial neuropil, the posterolateral protocerebrum, and the column. All of these neuropils are the target areas of AL PNs (Ian, Zhao, et al., 2016). In contrary to the mushroom bodies, the lateral protocerebrum is not assumed to be involved in memory and learning, but has been associated with experience-independent behavior, such as courtship and upwind walking and flying (de Belle & Heisenberg, 1994; Heimbeck, Bugnon, Gendre, Keller, & Stocker, 2001; Kido & Ito, 2002; McBride et al., 1999).

1.2 Calcium imaging

Taking use of calcium as an intracellular messenger, enables us to investigate neural activity at a population level through calcium imaging. At resting levels, neurons have an intracellular calcium concentration of approximately 100 nM; during activity however, these levels can reach 1000 nM (Berridge, Lipp, & Bootman, 2000), making intracellular calcium concentration a good indicator for neural activity, as the fluorescence changes during calcium imaging are shown to be a result of calcium influx/outflux in an excited or inhibited neuron (Kerr, Greenberg, & Helmchen, 2005). Calcium imaging requires the use of calcium indicators, measuring the amount of free intracellular calcium ions (Grienberger & Konnerth, 2012). Chemical calcium indicators are a combination of calcium chelator, which induces an intramolecular structural change when binding to a calcium ion, and a fluorophore which emits light when exited by light at a given wavelength. So, when the calcium indicator binds to a calcium ion, a structural change occurs that leads to the change of the wavelength at which this calcium indicators are maximally exited. The ratiometric calcium indicator Fura-2 dextran, used in this project, is maximally exited at ~380 nm when it is not bound to a calcium ion. However, when the calcium indicator is bound to a calcium ion, the calcium indicator is maximally exited at a wavelength of ~340 nm (Tsien, 1989). The possibility of the ratiometric measurements on the base of fluorescent intensities for these two excitation wavelengths makes it advantageous for correction of artifacts being caused by bleaching, variation of light intensities, and changes in focus. Although calcium imaging has been a common technique to indirectly measure the activity in the AL, several approaches exist. The most common technique has probably been bath application, which has the advantage of being noninvasive, and do not require a lot of time. However, this method requires the use of membrane-permeable dye, which will result in this dye being present in all tissue. Which in turn mainly leads to recording of the calcium changes in the OSN afferents. The fact that Fura-2 dextran is a membrane-impermeable calcium indicator, makes it possible to stain a distinct population of neurons by applying the dye into a specific area, in our case the calyces. The dye is then transported (retrogradely in this instance) to the location of interest – here, the particular categories of AL glomeruli.

1.3 Aims

The current study aims to explore functional characteristics of the MGC and PCx glomeruli applying calcium imaging of the primarily uniglomerular PNs confined to the medial ALT. Odor evoked calcium fluctuations will be registered in response to the principal pheromone components (Z11-16:ald and Z9-16:ald), four minor pheromone components (tetradecenal (14:ald), *cis-7*-hexadecenal (Z7-16:ald), *nonanal* (9:ald), *heptanal* (7:ald)) and two interspecific components (Z9-14:ald and Z11-16:OH). In order to investigate mixture interactions within glomeruli in the MGC and PCx different blends of these components, will be applied as well.

Specific aims:

1. To achieve successful retrograde staining of the uniglomerular PNs confined to the medial ALT.
2. To obtain appropriate amount of data suitable for consequent analysis.
3. To process data in KNIME for mapping of glomeruli and in R/Matlab for the visualization of time traces.
4. Statistical analysis of obtained data.

2 Materials and methods

2.1 The insects

Male moths of the species *H. armigera* (Lepidoptera: Noctuidae, Heliothinae) were used in this study. The pupae were provided by Henan Jiyuan Baiyun industry Co,Ltd. in China. Both pupae and hatched moths were kept in a climate chamber at 24±1°C, with 70% humidity, and had a day-night cycle of 14-10 hours. The hatched moths were kept in cylindrical containers (diameter = 12.5 cm, height = 20 cm), with a maximum of eight insects in each cylinder to avoid space related stress. Each cylinder was equipped with *ad libitum* access to a 10% sucrose solution.

2.2 Insect preparation

Before preparation, the moth was kept in the refrigerator at 4 °C for 15-30 minutes for sedation. Then, the moth was gently retained in a plastic tube, while making sure not to injure the antennae. The head was left exposed, and fixated with dental wax (Kerr, Orthodontic Tray Wax) to keep it stable. All further preparation was done under a stereomicroscope (Leica DMC 4500). First, scales were gently removed from the head with forceps. Then, the head capsule was opened with a razor-blade knife above the dorso-posterior part of the brain allowing an easy access to the calyces. After removing the trachea and a fine sheet covering the brain, a small hole was made just anterior to the calyces using fine forceps, to enable easier penetration with the glass electrode for dye application. Depending on the amount of dye on each electrode, up to four of them were used for a successful staining of the medial ALT. Application with ringer solution (in mM: 150 NaCl, 3 CaCl2, 2 KCl, 25 sucrose, and 10 N-tris (hydroxymethyl)-methyl-2-amino-ethanesulfonic acid, pH 6.9) kept the brain moist. The ringer solution was also used to rinse the brain 3-5 times after staining, mitigating the amount of redundant dye. After staining, the moth was kept in a humid box at 4 ºC over night, allowing for retrograde transport of the fluorescent dye from the calyces to the AL. Finally, on the recording day, the anterior part of the head capsule was removed to give access to the AL from a dorsal view. Finally, the antennae were fixated with eicosane (Sigma-Aldrich). No harm is inflicted upon the insect's antennae during the application of eicosane due to its low melting point.

The glass electrodes were made using a micropipette puller from SUTTER INSTRUMENT CO. MODEL P-97. Dye was manually applied to the electrode by mixing

crystals of Fura-2 dextran (10,000 MW, in 2% BSA; Molecular Probes) with 1 µl of distilled water on a glass plate.

2.3 Odor stimulation

All female-produced compounds used in this study (Table 1) were provided by Pherobank, Wijk bij Duurstede, the Netherlands. The pheromone stimuli included the primary and secondary pheromone component of H. armigera, *cis-11-hexadecenal* (Z11-16:ald) and *cis-9-hexadecenal* (Z9-16:ald), plus minor components produced by the female, *tetradecenal* (14:ald), *cis-7-hexadecenal* (Z7-16:ald), *nonanal* (9:ald), *heptanal* (7:ald) and two interspecific components known to be sexually behaviorally relevant for H. armigera, *cis-9-tetradecenal* (Z9-14:ald) and *cis-11-hexadecenol* (Z11-16:OH). The stimuli are divided into the following categories: principal pheromone components, interspecific components, component blends, minor pheromone components, and control (Table 1). In addition, for optimizing glomerular mapping during the data processing phase, headspace of sunflower was used at the end of each stimulus sequence. Mineral oil (Across Organics) was used as a solvent for all the pheromones except for pheromone E, which turned out not to be soluble in mineral oil. Therefore, for this pheromone, n-hexane (VWR Chemicals) was used as solvent. Hexane, however, elicits a stronger response than the mineral oil. For this reason, an additional control with hexane was required in the stimuli sequence where pheromone E was included.

20 µl of a stimulus was applied on the filter paper placed into a 150 mm glass Pasteur pipette. Which corresponds to a total 20 µg stimuli for concentration 10^{-3} and 200 ng for concentration 10^{-5}. The pheromone blends were mixed before the application, and the total amount of the mixture is equal to the amount of a single component. When not in use, the stimulus pipettes sealed with parafilm were stored at -18 °C.

Table 1: List of stimuli used in the project, their coding names, and solvents.

	Stimuli		Code	Solvent
Principal pheromone components	Primary pheromone	Z11-16:Ald	A	Mineral oil
	Secondary pheromone	Z9-16:Ald	B	Mineral oil
Interspecific components	Interspecific	Z9-14:Ald	C	Mineral oil
	Interspecific	Z9-16:OH	D	Mineral oil
Component blends	Natural blend 97.5:2.5	Z11-16:Ald + Z9-16:Ald	ABn	Mineral oil
	50:50 blend	Z11-16:Ald + Z9-16:Ald	AB	Mineral oil
	50:50 blend	Z9-14:Ald + Z9-16:OH	CD	Mineral oil
	50:50 mix between the ABn blend and the CD blend	Z11-16:Ald + Z9-16:Ald + Z9-14:Ald + Z9-16:OH	ABCD	Mineral oil
Minor pheromone components	Minor pheromone	14:Ald	E	Hexane
	Minor pheromone	Z7-16:Ald	F	Mineral oil
	Minor pheromone	9:Ald	G	Mineral oil
	Minor pheromone	7:Ald	H	Mineral oil
	Control	Mineral oil	Con	
	Control	Hexane	Hex	
	Sunflower	Sunflower headspace		

The airflow and stimulation time during imaging were controlled by a stimulus controller (SYNTECH CS-55), which ensured that there was a constant airflow through a PTFE tube, pointing at the antenna ipsilaterally to the AL of interest. The tube with constant humidified airflow was placed approximately 3 cm from the antenna. The stimulus pipette was inserted orthogonally to the tube that provided constant airflow. The stimulation onset was set to 3 seconds after the imaging started and lasted for 2 seconds. Each stimulation was repeated two times and an inter-stimulus interval of 1 minute was kept to avoid adaptation. The stimulus concentration was kept the same for each subject, meaning that only one concentration was tested on each individual. Table 2 gives an overview of stimuli and concentrations used. Each stimulation sequence was randomized, but the first and the last stimulation was always a control stimulus.

Tabell 2. Overview of stimuli and concentrations used on each test subject. Green represents stimuli which were tested, whereas, pink represents stimuli that were not tested.

Subject #	Concentration	A	B	C	D	AB	ABn	CD	ABCD	E	F	G	H
1	10^{-3}												
2	10^{-3}												
3	10^{-3}												
4	10^{-3}												
5	10^{-3}												
6	10^{-3}												
7	10^{-3}												
8	10^{-5}												
9	10^{-5}												
10	10^{-5}												
11	10^{-5}												
12	10^{-5}												
13	10^{-5}												
14	10^{-5}												

2.4 Imaging

The moth was placed under an epifluorescent microscope (Olympus BX51WI), in a position allowing for excitation and imaging of the dorso-posterior part of the AL. The microscope was equipped with a 20x/1.00 water immersion objective (XlUMPlanFL N), and ringer solution enclosed the area between the preparation and the objective during imaging. Recordings were performed using a CMOS camera (Hamamatsu ORCA-Flash 4.0 V2 C11440-22CU). A polychromator (TILL Photonics Polychromatro V) excited the preparation with a 340 nm and 380 nm wavelength light at regular intervals. To secure the separation of excitation light (340/380 nm) and the emission light (peak at 505/520 nm), a dichroic mirror was used along with an emission filter (490-530). Recordings were acquired using Live Acquisition V2.6.0.35 (TILL Photonics) accompanying a TILL Photonics imaging control unit. Image binning-size was set to 4x4 and the recordings lasted for 10 seconds with 100 frames, resulting in 100 ms in each frame.

2.5 Data processing and Statistical analysis

The raw data gathered from imaging was processed in KNIME Analytics Platform 2.12.2, with the ImageBee plugin (Figure 4) (Strauch, Rein, Lutz, & Galizia, 2013). After initial reading of

the images, a between movie stabilization was done to rectify for potential drift in the image, correcting for a maximum of 30 pixels. The data was processed within two paths, the first one including creation of an AL map with identifiable glomeruli (the upper path in Figure 4). To create an AL map, a Z-score normalization was performed on the data set, using the mean and standard deviation for each separate movie, before a gaussian filter with kernel size 5 was applied. The movies were then run through a principal component analysis algorithm, which identifies neighboring pixels that have similar response patterns, laying the foundation for identification of glomeruli. The data was smoothened by a new gaussian filter kernel size 9. Then, a convexcone algorithm was used to find the areas with the highest correlations, called regions of interest (ROI), and present it as a map. The number of ROIs was decided through trial and error identifying the highest number of glomeruli, yet not causing it to divide a glomerulus into two ROIs. ROIs that did not represent a glomerulus were manually removed from the AL map.

In the other path, a baseline activity was created for each pixel, using the mean of frame number 10-30, and subtracting it from the rest of the data. This resulted in a baseline set to zero, and all responses could thus be presented as changes relative to the baseline. Finally, the AL map were merged with the movie containing the baseline data, projecting a movie onto each ROIs and creating time-series for each glomerulus that could be written out in a .csv format for further analysis. A list of all stimuli used was also written out in .csv format.

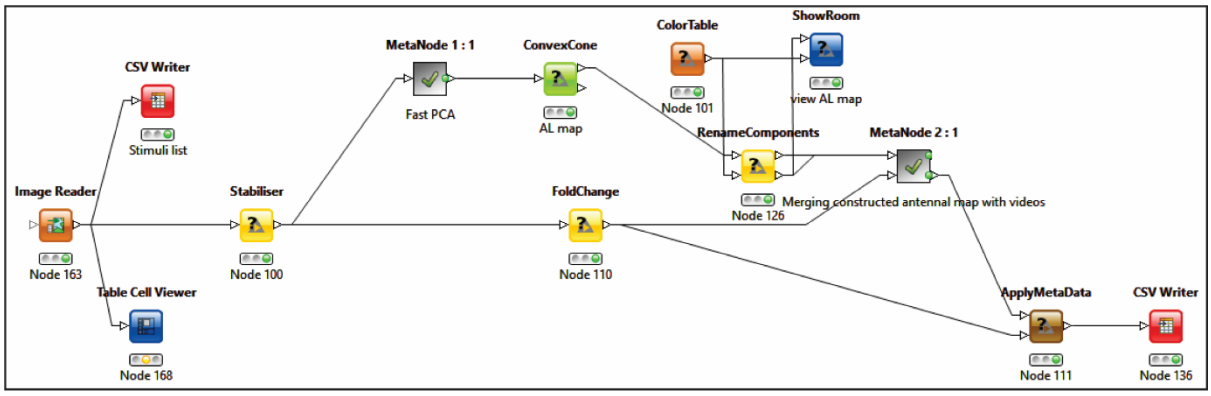

Figure 4. Flowchart of the ImageBee plugin in KNIME.

R-studio (1.1.463) was used to create single glomerular traces for preliminary examination of each individual subject, as well as creating an excel output file where the ROI time-series and the stimulus list was combined, which was better suited for further analysis.

A series of paired sample t-test comparing the response strength between the control and each stimulus was performed using the statistical software Jasp (0.9.2.0). The response strength was defined as the highest response between frame #20 and 40 for each stimulus. Additionally, paired sample t-test was also performed between the stimulus that were significantly different from the control; for instance, if stimulus B and C elicited a response significantly different from the control, a t-test was also performed between stimulus B and C, checking if there is a significant difference in response to these stimuli. Throughout the statistical testing 0.05 was used as the cut of level for significance. For statistical analysis of responses evoked by the principal pheromone component, the interspecific components, and the component blends, only subjects which is stimulated with all of these stimuli are included (subject #3-9). Statistical analysis of responses to the minor pheromone component were performed as well, for them, all available data is used (subject #10-14). During all tests where stimuli responses are compared with control responses, hexane is used as a control for pheromone E, whereas all others are compared to the mineral oil control. The effect size presented in the result section is Cohen's d_z, and is calculated the following way: $d_z = t / \sqrt{n}$. Where the t is the t-value of the t-test, and the n is the number of subjects.

Calcium traces presented in the result section were made using matlab (R2018b). Mean calcium traces with standard error are made using all data, comparing each stimulus evoked response to the control response. Additionally, mean calcium traces are also made exclusively for the subjects included in the statistical analysis. In these traces, the component blends are plotted against the single component constituting the blends. A comparison of responses across concentration were also performed for stimuli A-D. These was compared by plotting the two concentrations against each other using pure responses. The pure responses were deduced by subtracting the control response from the stimulus response.

All figures in this thesis were made using adobe illustrator (1.0) and/or adobe photoshop (20.0.4).

2.6 Data Cleaning

The original calcium imaging protocol, as described above, lasts for a total of 10 seconds and has 100 frames, resulting in 100 ms in each frame. However, this protocol was not followed for the first four preparations (ID#1-4) included in the analyses. For these preparations, the total time cycle varies from 11.3 seconds to 14.1 seconds. Although, the number of frames

stayed the same, resulting in 113-141 ms in each frame. The onset of odor stimulation was still fixed to 3 seconds after imaging started and lasted for 2 seconds. This combination created complications in quantifying the data, because the stimulation period for each preparation started at different frames and lasted for different number of frames (Figure 5). This was solved by calculating the onset frame of each of the subjects and aligning them (using excel) so that the stimulus onset occurred at frame number 20 for the entire dataset. Because of this, the total frame length of the data is reduced by 10 frames. Although this accounts for the stimulus onset, the number of stimulus frames after onset still varies from 14 to 18 frames in subject ID#1-4, compared to the 20 frames of the original protocol. However, this aligning should make the data more comparable, although, keeping in mind that the stimulus starts at frame 20 and lasts for 14 to 20 frames.

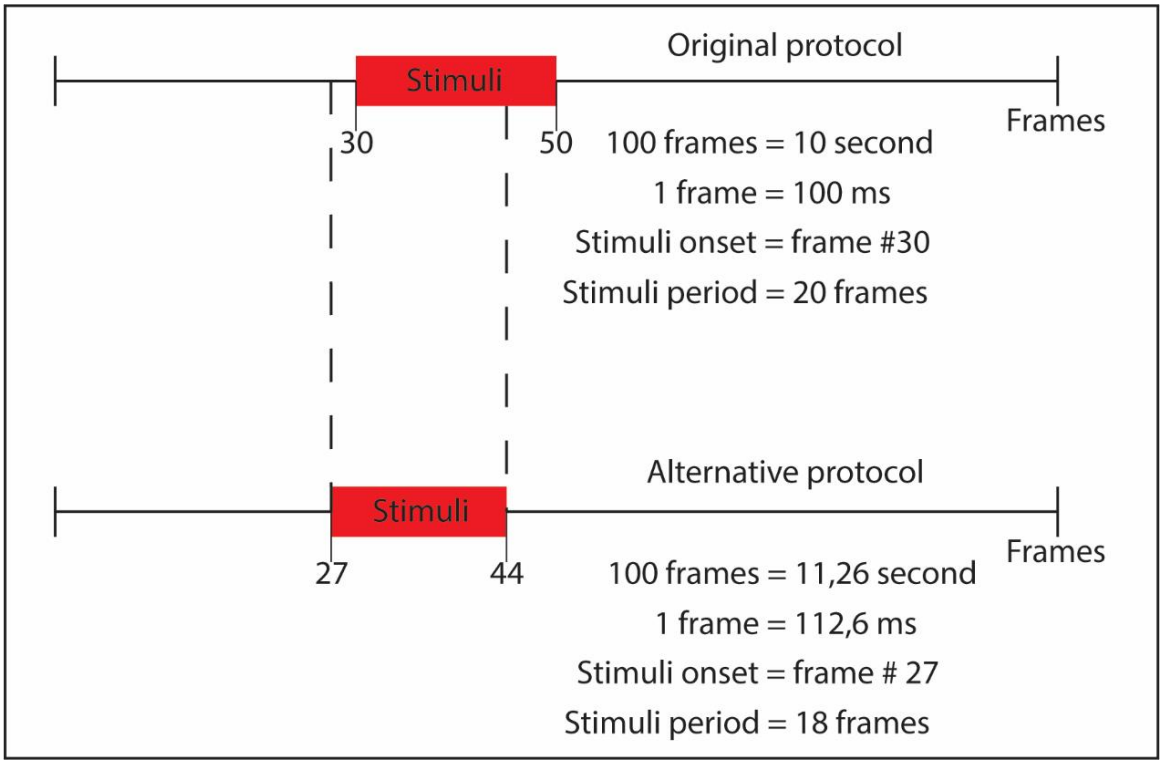

Figure 5. Comparison of original and alternative protocols.

2.7 Ethics

There are no restrictions in the laws for the use of Lepidoptera in research, as they are not included in the *Regulation of use of animals in research trials.* Although, awareness was made to give the insects an ethically treatment, making sure not to case any unnecessary harm or distress.

3 Results

A total of 42 experimental datasets completed the full procedure of staining, imaging, and processing in KNIME. For further analysis, the dataset had to have successfully labelled AL glomeruli making it possible to generate an AL-map where the PCx and/or the MGC glomeruli were recognizable. The response pattern of the MGC also had to be non-global, ensuring that there was no cross contamination during stimulation. A total of 14 datasets met these criteria and are presented here in the results. All MGC glomeruli were identified in 13 of these, whereas in subject #13, the cumulus could not be identified.

Time traces presented here demonstrate the odor-evoked activity in the two distinct AL sub-areas, the MGC and the PCx. The results are presented in the following order: the MGC (glomerulus by glomerulus), the PCx, and finally, a comparison of responses to stimuli of different concentrations. For the comparison of response strength between the control and each stimulus, the significant responses are presented in the text, while a complete table of both significant and non-significant results are added in the extra material.

3.1 MGC glomeruli responses

3.1.1 Odor-evoked responses in the Cumulus

The traces for the cumulus demonstrate the strongest activation to the primary pheromone, A, as well as any component blend that incorporates the primary pheromone (AB, ABn, ABCD) (Figure 6). Weaker activations can be seen when stimulating with the interspecific components C and D.

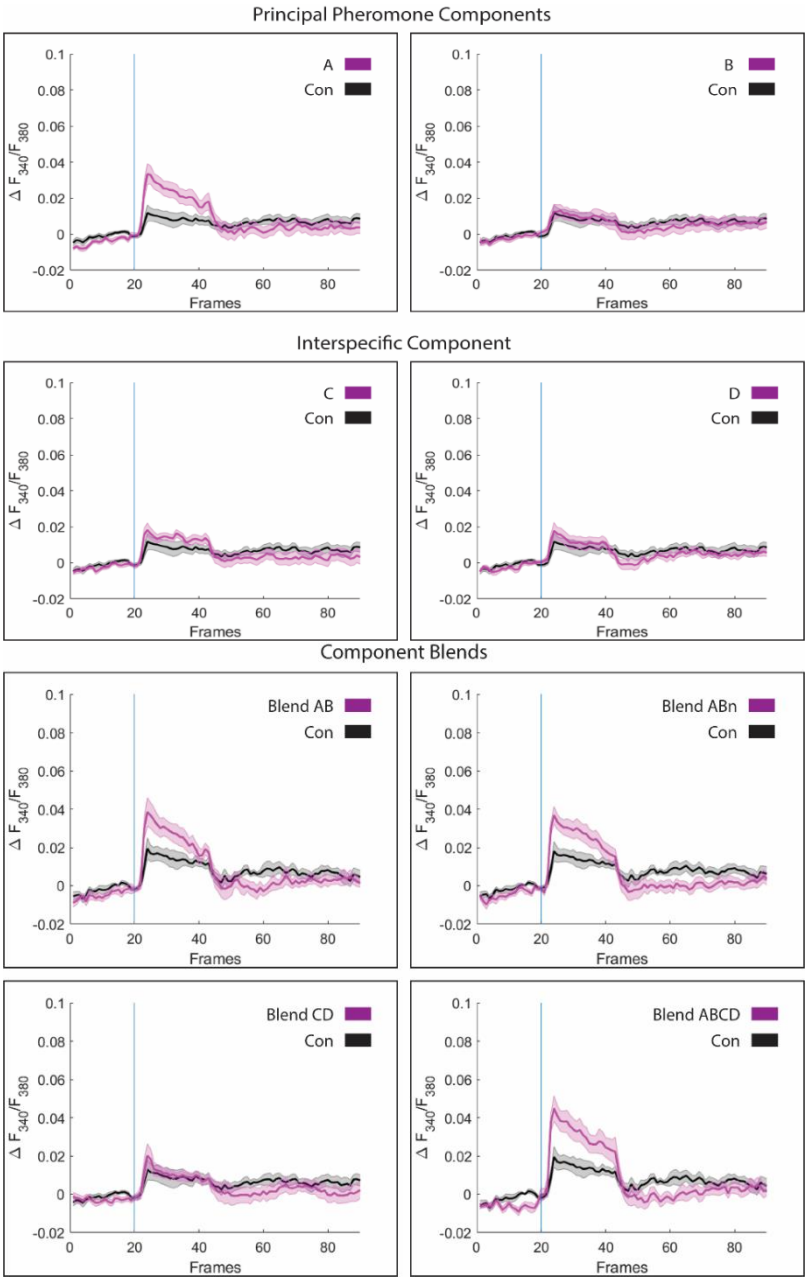

Figure 6. Mean ± SE calcium traces of the Cumulus during stimulation with A (Z11-16:Ald) (n=13), B (Z9-16:Ald) (n=13), C (Z9-14:Ald) (n=13), D (Z9-16:OH) (n=13), AB (50:50 blend) (n=8), ABn (97.5:2.5 blend) (n=9), CD (50:50 blend) (n=10), and ABCD (50:50 blend of ABn and CD) (n=8). Each stimulus is presented twice. The blue vertical line represents the stimulus onset at frame 20. Con, control.

In total, four stimuli had a response strength significantly different from the control response (*M*= 0.025, *SD*= 0.013). As indicated above, the primary pheromone (*M* = 0.045, *SD* = 0.018), indeed elicits a cumulus response significantly stronger than the control, t(6) = 5.516, p = 0.001, d = 2.085. A response significantly stronger than the control was also found stimulating with the component blends, AB (*M* = 0.044, *SD* = 0.019), ABn (*M* = 0.042, *SD* = 0.012), and ABCD (*M* = 0.049, *SD* = 0.018), AB: t(6) = 4.522, p = 0.004, d = 1.709. ABn: t(6) = 4.059, p = 0.007, d = 1.534. ABCD: t(6) = 5.366, p = 0.002, d = 2.028. While stimuli lacking the primary pheromone, including the secondary pheromone B, the interspecific components C and D, and the component blend CD, did not elicit significant responses (p>0.2).

Traces for the same individuals are presented in Figure 7. When plotting the responses to stimuli A, AB, ABn, and ABCD against each other, only small differences can be observed, although component blend ABCD elicits a slightly stronger response than both stimuli A, AB and ABn. However, a paired sample t-tests of all the significant responses, reveal that only ABCD and ABn is statistically different from each other, t(6) = 2.631, p = 0.039, d = 0.994.

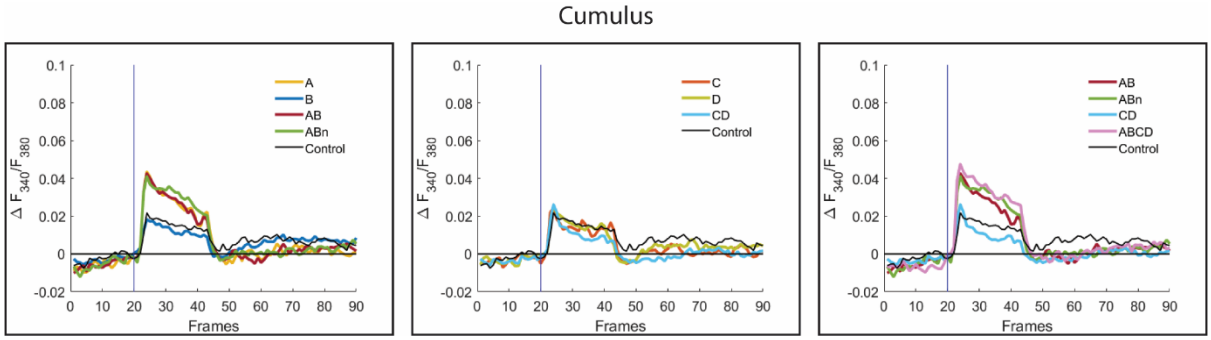

Figure 7. Mean calcium traces of the Cumulus for subjects #3-9. The responses to the blends are plotted against their constituents' responses and the control. The blue vertical line represents the stimulus onset at frame 20. Stimuli used: A (Z11-16:Ald), B (Z9-16:Ald), C (Z9-14:Ald), D (Z9-16:OH), AB (50:50 blend), ABn (97.5:2.5 blend), CD (50:50 blend), and ABCD (50:50 blend of ABn and CD).

Traces for the minor pheromone components are presented in Figure 8. No significant difference in response strength to stimuli E-H and the control was found (ps> 0.204) in the subjects tested (#10-12 and 14).

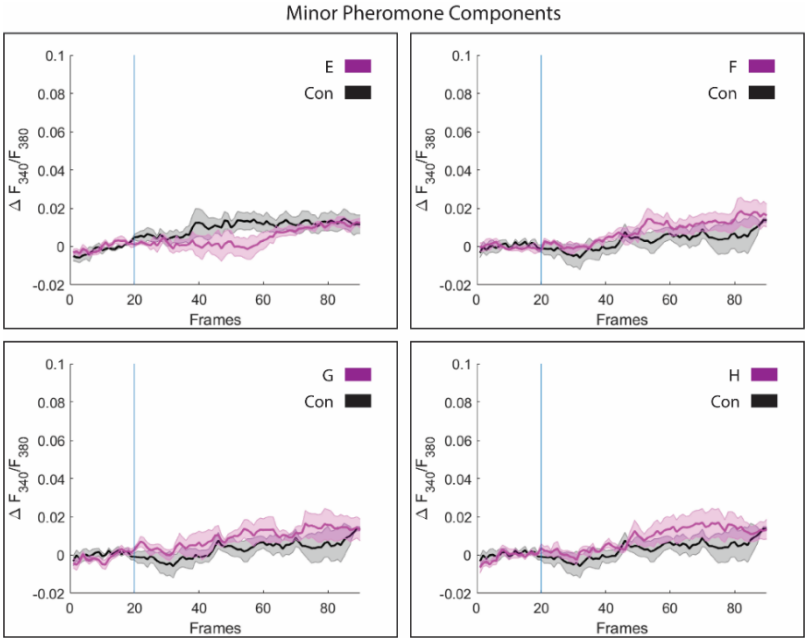

Figure 8. Mean + SE calcium traces of the Cumulus during stimulation with minor pheromone components E (14:Ald) (n=4), F (Z7-16:Ald) (n=4), G (9:Ald) (n=4), and H (7:Ald) (n=4). Each stimulus is presented twice. The blue vertical line represents the stimuli onset at frame 20.

3.1.2 Odor-evoked responses in the small MGC-unit located anteriorly, DMA

Stimulation with the interspecific components, C and D, induced a strong activation of the DMA (Figure 9). Mixtures including these components, such as CD and ABCD, also elicited strong activation (Figure 10). Each of the principal pheromone components, A and B, plus the pheromone blends, AB and ABn, induced smaller activation; the pheromone A and the blend AB show a transient excitation immediately after the stimulus onset (Figure 9 and 10).

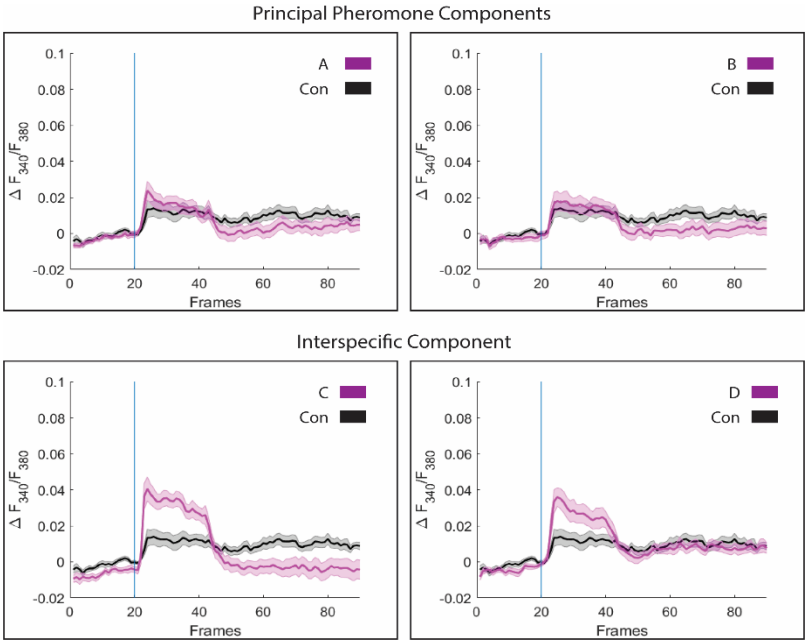

Figure 9. Mean ± SE calcium traces of the DMA during stimulation with A (Z11-16:Ald) (n=14), B (Z9-16:Ald) (n=14), C (Z9-14:Ald) (n=14), D (Z9-16:OH) (n=14). Each stimulus is presented twice. The blue vertical line represents the stimulus onset at frame 20.

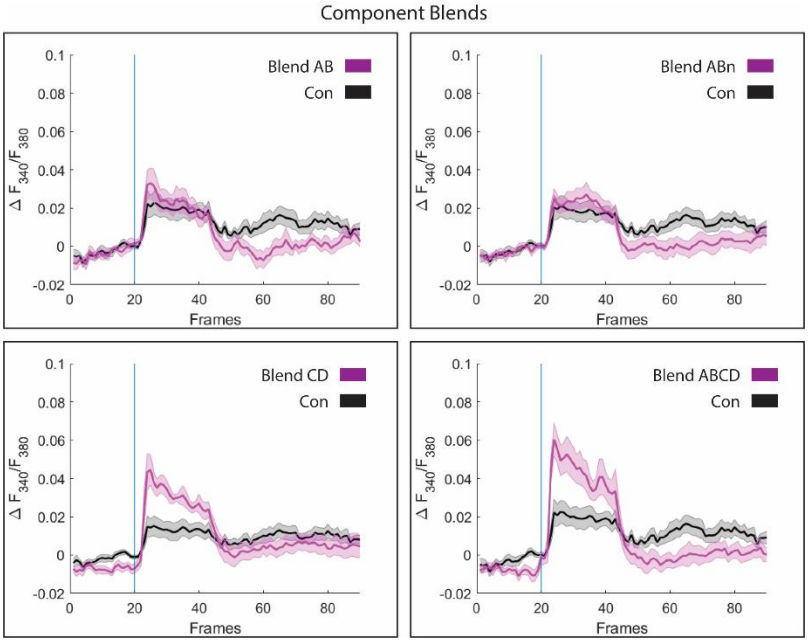

Figure 10. Mean ± SE calcium traces of the Cumulus during stimulation with AB (50:50 blend) (n=8), ABn (97.5:2.5 blend) (n=9), CD (50:50 blend) (n=11), and ABCD (50:50 blend of ABn and CD) (n=8). Each stimulus is presented twice. The blue vertical line represents the stimulus onset at frame 20.

Compared to the response strength of the control (M = 0.031, SD = 0.016), both interspecific components, C (M = 0.059, SD = 0.014) and D (M = 0.053, SD = 0.02) elicited significant responses, C: $t(6) = 8.979$, $p < 0.001$, $d = 3.394$, D: $t(6) = 7.785$, $p < 0.001$, $d = 2.942$. Likewise, component mixtures including the interspecific compounds, such as CD (M = 0.061, SD 0.025) and ABCD (M = 0.066, SD 0.023), also evoked significant responses in the DMA, CD: $t(6) = 4.425$, $p = 0.004$, $d = 1.672$, ABCD: $t(6) = 6.771$, $p < 0.001$, $d = 2.559$. The responses to each of the principal pheromone components and the pheromone blends (AB and ABn) were not significantly different from the control response ($p > 0.07$). Figure 11 also shows that the stimulus-evoked activations that were statistically different from activation during control (C, D, CD, and ABCD) are quite different in response strength. Indeed, a comparison of time traces corresponding to these responses shows that the DMA response to the component blend ABCD is significantly stronger than the response to stimulus D alone, $t(6) = 3.221$, $p = 0.018$, $d = 1.218$. Generally, the responses to the single interspecific components and the component mixture, CD, seem to be more transient as compared to the response to ABCD (Figure 11).

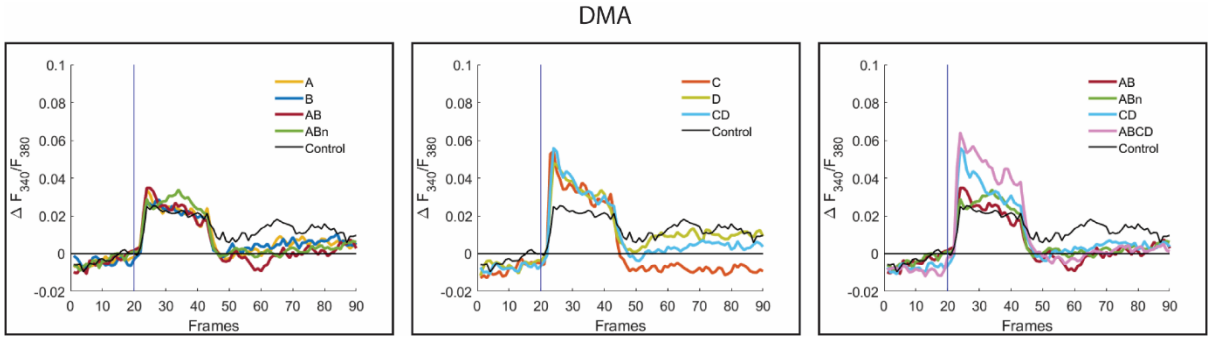

Figure 11. Mean calcium traces of the DMA for subjects #3-9. The responses to the blends are plotted against their constituents' responses and the control. The blue vertical line represents the stimulus onset at frame 20. Stimuli used: A (Z11-16:Ald), B (Z9-16:Ald), C (Z9-14:Ald), D (Z9-16:OH), AB (50:50 blend), ABn (97.5:2.5 blend), CD (50:50 blend), and ABCD (50:50 blend of ABn and CD).

By looking at the traces, none of the minor pheromone components seems to evoke any clear activity in the DMA (Figure 12). A paired sample t-test, however, showed that stimulus G (M = 0.014, SD = 0.005) have a significantly stronger response than the activation during control (M = 0.007, SD = 0.006), t(4) = 3.110, p = 0.036, d = 1.391. The minor pheromone components E, F, and H, on the other hand, did not evoke statistically significant responses (ps> 0.36).

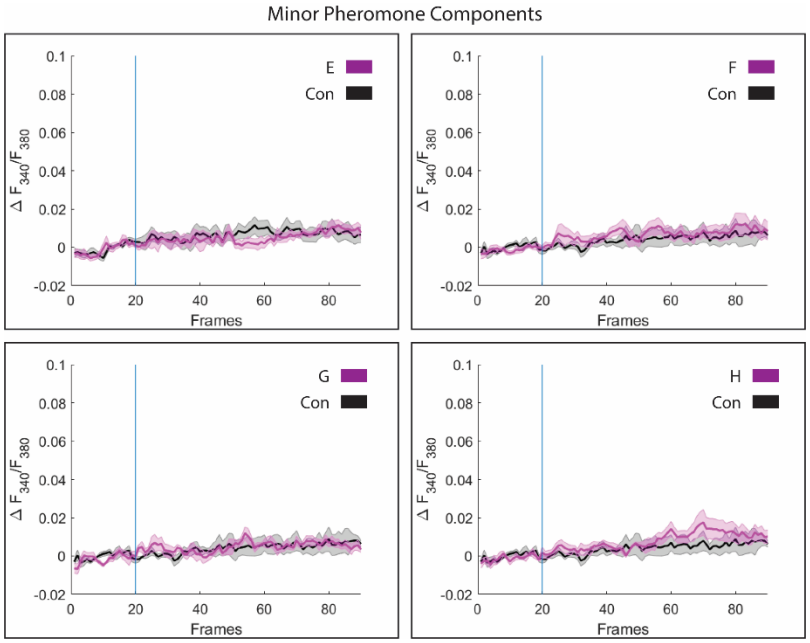

Figure 12. Mean + SE calcium traces of the DMA during stimulation with minor pheromone components E (14:Ald) (n=5), F (Z7-16:Ald) (n=5), G (9:Ald) (n=5), and H (7:Ald) (n=5). Each stimulus is presented twice. The blue vertical line represents the stimuli onset at frame 20.

3.1.3 Odor-evoked responses in the small MGC-unit located posteriorly, DMP

The DMP was activated by a wide variety of the stimuli tested (Figure 13). While single components B and C induced strong excitation, the primary pheromone A only elicits a transient activation of the DMP. Furthermore, all component blends also evoked higher activity than what the control stimulus did, although the strongest activity looks to be observed during stimulation with the blend ABCD, followed by stimuli AB and CD.

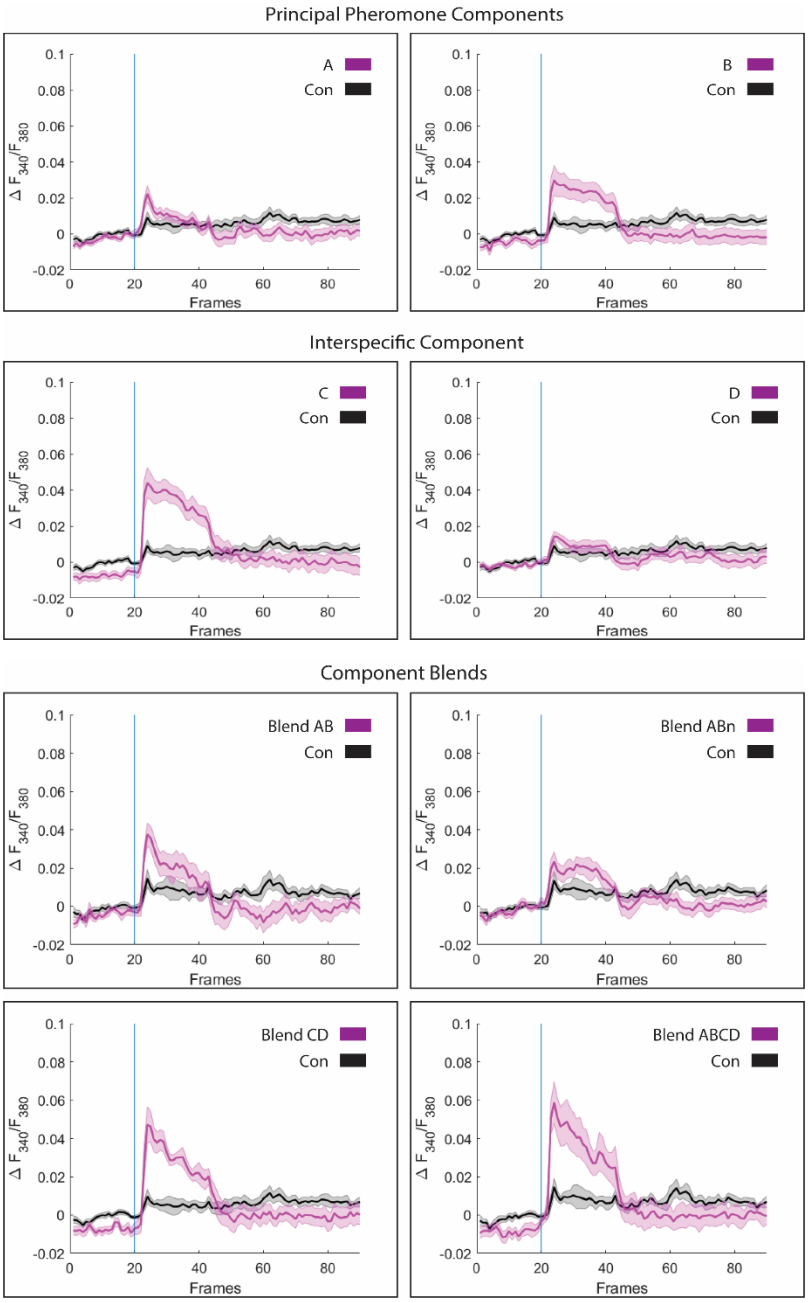

Figure 13. Mean ± SE calcium traces of the DMP during stimulation with A (Z11-16:Ald) (n=14), B (Z9-16:Ald) (n=14), C (Z9-14:Ald) (n=14), D (Z9-16:OH) (n=14), AB (50:50 blend) (n=8), ABn (97.5:2.5 blend) (n=9), CD (50:50 blend) (n=11), and ABCD (50:50 blend of ABn and CD) (n=8). Each stimulus is presented twice. The blue vertical line represents the stimulus onset at frame 20.

A series of paired sample t-tests found responses significantly different from the activation during control (M = 0.022, SD = 0.013) to six different stimuli in the DMP. Of the single components, both the principal pheromone component A (M = 0.035, SD = 0.017) and B (M = 0.053, SD = 0.029), in addition to the interspecific component C (M = 0.064, SD = 0.028) elicited statistically significant responses, A: $t(6) = 3.189$, $p = 0.019$, $d = 1.205$, B: $t(6) = 4.59$, $p = 0.01$, $d = 1.399$, C: $t(6) = 4.59$, $p = 0.004$, $d = 1.735$. Likewise, the three component blends AB (M = 0.042, SD = 0.02), CD (M = 0.06, SD = 0.028), and ABCD (M = 0.065, SD = 0.032) also elicited significant responses in the DMP, AB: $t(6) = 3.481$, $p = 0.013$, $d = 1.316$, CD: $t(6) = 4.119$, $p = 0.006$, $d = 1.557$, ABCD: $t(6) = 4.776$, $p = 0.003$, $d = 1.805$. Stimuli D and ABn, on the other hand, was not significantly different from the control ($p > 0.094$).

Although the primary pheromone, A, elicited a response statistically different from the control response, we can see from the mean traces in Figure 14 that the response is transient and lasts only a few frames. Moreover, although the activation strength when stimulating with ABn was not significantly different from the control, the traces show a clear difference in the activity pattern (Figure 14).

Not only did six of the stimuli elicit significant responses in the DMP, but significant differences between these responses were observed as well. Both stimuli B, C, CD, and ABCD induce responses significantly stronger than the responses induced by stimulus A, B: $t(6) = 3.183$, $p = 0.019$, $d = 1.203$, C: $t(6) = 3.376$, $p = 0.015$, $d = 1.276$, CD: $t(6) = 2.961$, $p = 0.025$, $d = 1.119$, ABCD: $t(6) = 4.070$, $p = 0.007$, $d = 1.538$. Additionally, the responses to component blend ABCD, is significantly stronger than the responses to the secondary pheromone component, B, $t(6) = 3.402$, $p = 0.014$, $d = 1.286$.

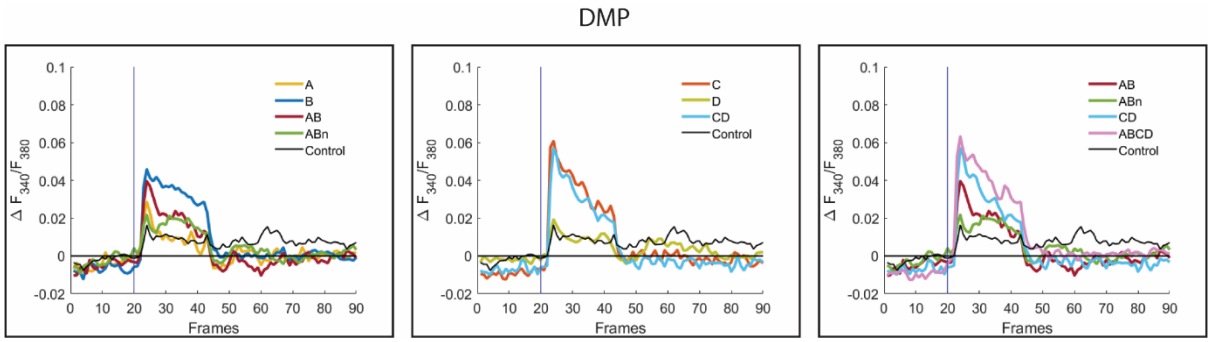

Figure 14. Mean calcium traces of the DMP for subjects #3-9. The responses to the blends are plotted against their constituents' responses and the control. The blue vertical line represents the stimulus onset at frame 20. Stimuli used: A (Z11-16:Ald), B (Z9-16:Ald), C (Z9-14:Ald), D (Z9-16:OH), AB (50:50 blend), ABn (97.5:2.5 blend), CD (50:50 blend), and ABCD (50:50 blend of ABn and CD).

The minor pheromone components, E-H, did not elicit significant responses in DMP (ps> 0.078). However, the standard error shown in Figure 15 indicates an inconsistent response when stimulating with the minor pheromone component, F.

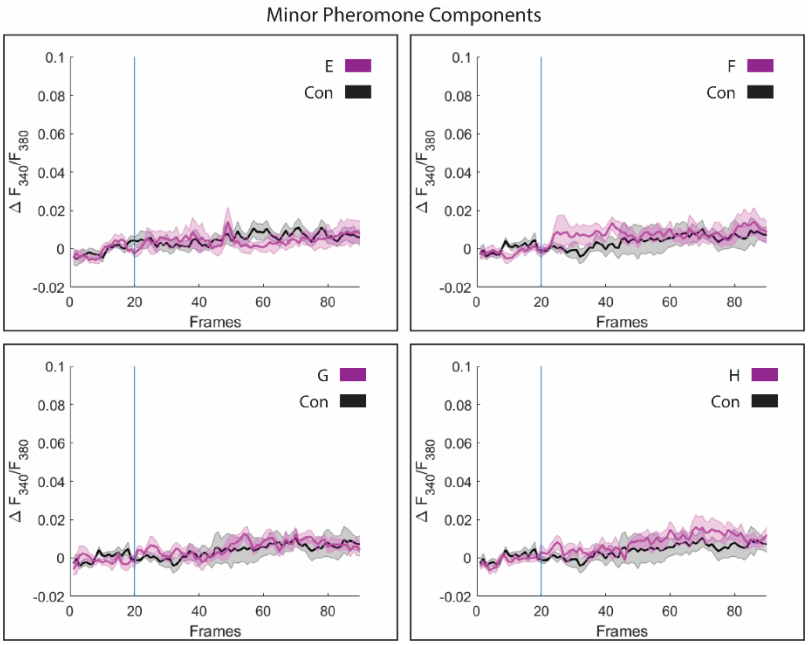

Figure 15. Mean + SE calcium traces of the DMP during stimulation with minor pheromone components E (14:Ald) (n=5), F (Z7-16:Ald) (n=5), G (9:Ald) (n=5), and H (7:Ald) (n=5). Each stimulus is presented twice. The blue vertical line represents the stimuli onset at frame 20

3.3 Odor-evoked responses in the posterior complex, PCx

In the 14 subjects, a total of 52 ROIs were identified as belonging to the PCx. However, while the MGC glomeruli are easily identifiable and provide a good landmark in the AL, the dorsally located PCx glomeruli, on the other hand, consist of ten glomeruli located at different focal planes (from a dorsal view) and are close to both the protocerebrum and the medial cell cluster. This makes it troublesome to identify the same PCx glomerulus across subjects; Figure 16 presents a good example of this. Thus, due to the impossibility to make a precise spatial recognition of the PCx glomeruli using this method, all glomeruli confined to the PCx were treated as one unite. Given that all the PCx glomeruli are grouped together and treated as one unite, we should expect an overall weaker response, as some glomeruli may respond to a given stimulus, while others do not.

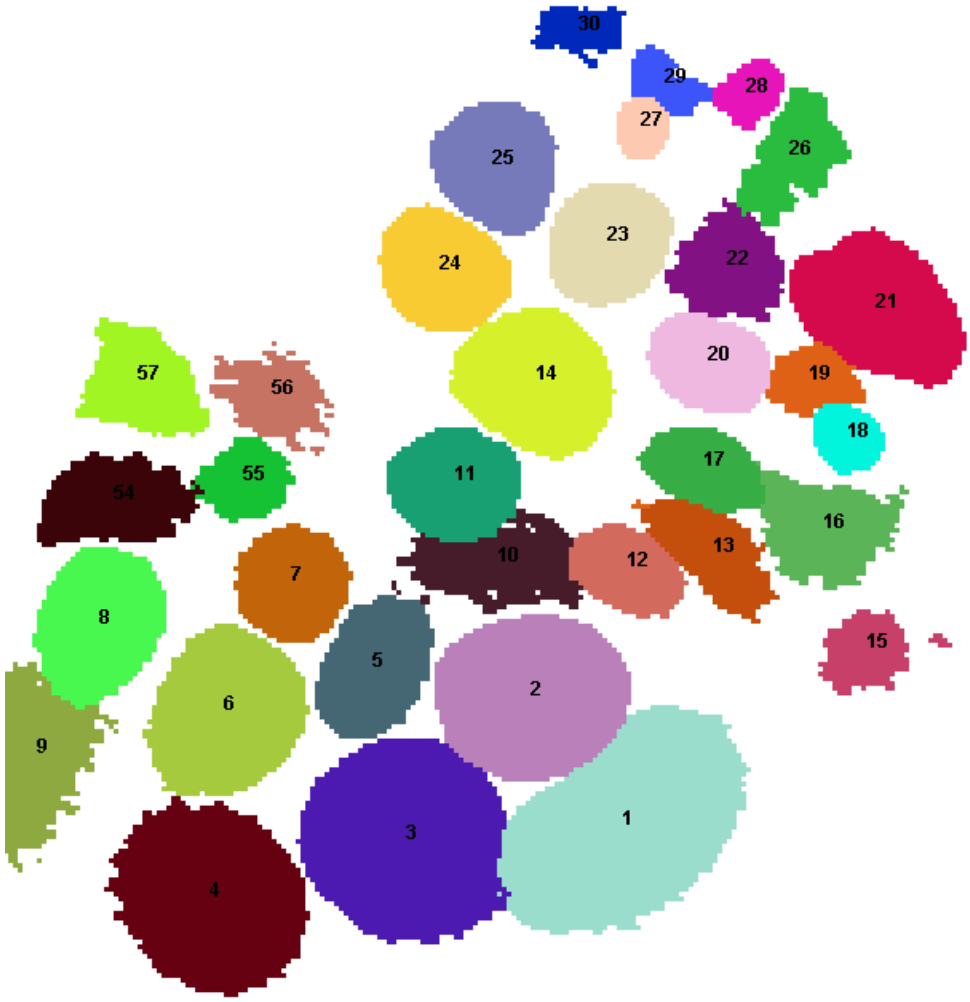

Figure 16. Automatically generated AL map demonstrating localization and identification of glomeruli. Glomerulus number 1= cumulus, 2=DMA, 3= DMP, 4-7= PCx, 8-9 and 54-57= unsure, 10-30= ordinary glomeruli.

Despite the fact that the ROIs are grouped together and treated as one unite, clear activity can be observed when stimulating with several of the stimuli as shown in Figure 17, where traces using all ROIs are presented. The strongest activation can be seen stimulating with the interspecific component, C, along with mixtures including C, i.e. CD and ABCD. However, weaker activations seem to be elicited by the other stimuli as well (Figure 17).

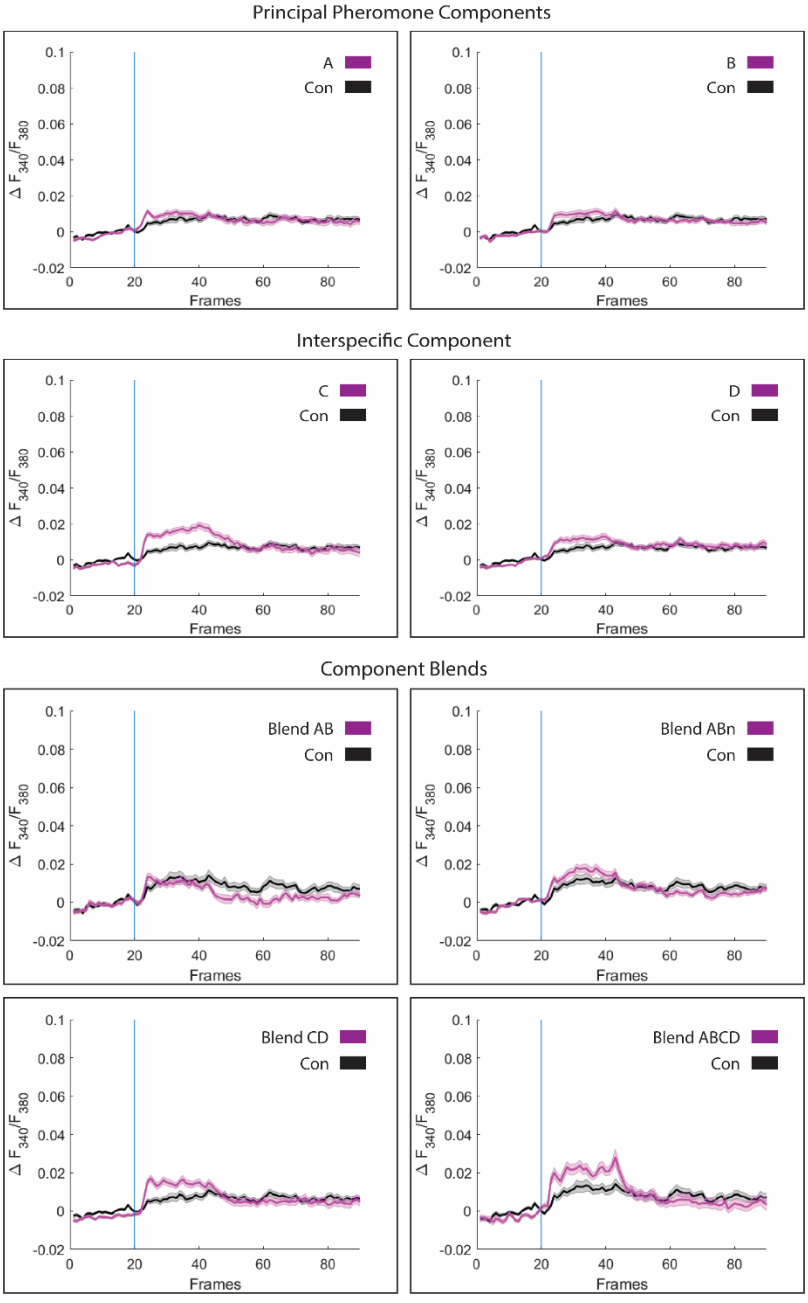

Figure 17. Mean ± SE calcium traces of the PCx during stimulation with A (Z11-16:Ald) (n=52), B (Z9-16:Ald) (n=52), C (Z9-14:Ald) (n=52), D (Z9-16:OH) (n=52), AB (50:50 blend) (n=26), ABn (97.5:2.5 blend) (n=30), CD (50:50 blend) (n=40), and ABCD (50:50 blend of ABn and CD) (n=26). Each stimulus is presented twice. The blue vertical line represents the stimulus onset at frame 20.

The t-test showed that stimuli ABn (M = 0.027, SD = 0.011), CD (M = 0.026, SD = 0.013), and ABCD (M = 0.031, SD = 0.014) induced responses significantly different from the control activation (M = 0.02, SD =0.014), ABn: t(22) = 2.719, p = 0.013, d = 0.567, CD: t(22) = 2.078, p = 0.05, d = 0.433, ABCD: t(22) = 3.956, p < 0.001, d = 0.825. In contrast, none of the interspecific components alone (C and D) elicited a significant response. Similarly, none of the principal pheromone components (A and B), or the pheromone blend AB, elicited significant responses (ps > 0.092). Both Figure 17, showing the full data, and Figure 18, showing data for subjects #3-9, display an unusual activity pattern for several of the stimuli, having a ‘’spike’’ in activity at the end of the stimulus period. Although it can be observed in the traces of several of the stimuli, it is most prominent in component blend ABCD.

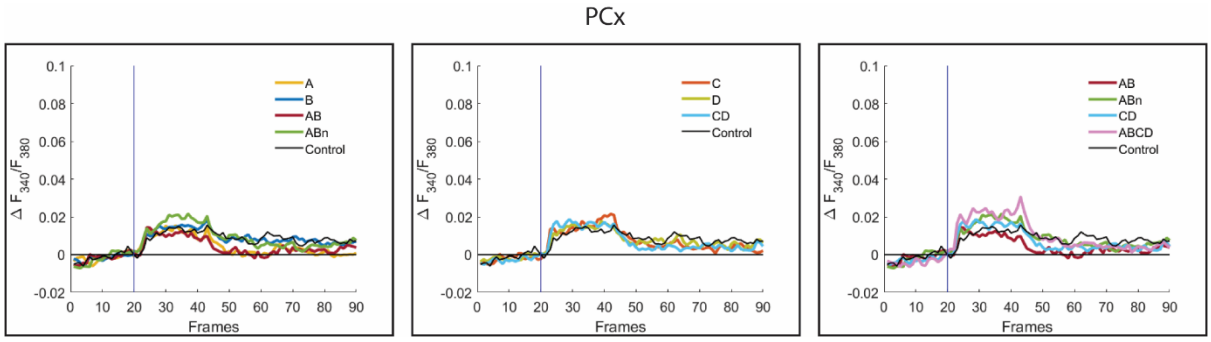

Figure 18. Mean calcium traces of the PCx for subjects #3-9. The responses to the blends are plotted against their constituents' responses and the control. The blue vertical line represents the stimulus onset at frame 20. Stimuli used: A (Z11-16:Ald), B (Z9-16:Ald), C (Z9-14:Ald), D (Z9-16:OH), AB (50:50 blend), ABn (97.5:2.5 blend), CD (50:50 blend), and ABCD (50:50 blend of ABn and CD).

Although the traces for the minor pheromone components did not indicate any clear excitation (Figure 19), all four stimuli elicited significant responses. Stimuli F (M = 0.012, SD = 0.007), G (M = 0.012, SD = 0.007), and H (M = 0.011, SD = 0.004), evoked responses significantly stronger than the mineral oil control (M = 0.008, SD = 0.003), F: t(22) = 2.483, p = 0.022, d = 0.529, G: t(22) = 2.671, p = 0.014, d = 0.570, H: t(22) = 4.174, p < 0.001, d= 0.890. The minor pheromone component E (M= 0.015, SD= 0.009), also elicited a response significantly stronger than its hexane control activation (M= 0.009, SD= 0.007), t(21) = 3.552, p = 0.002, d = 0.757. The traces for component E, however, also have a peculiar shape, being highest at the end of the stimulus period.

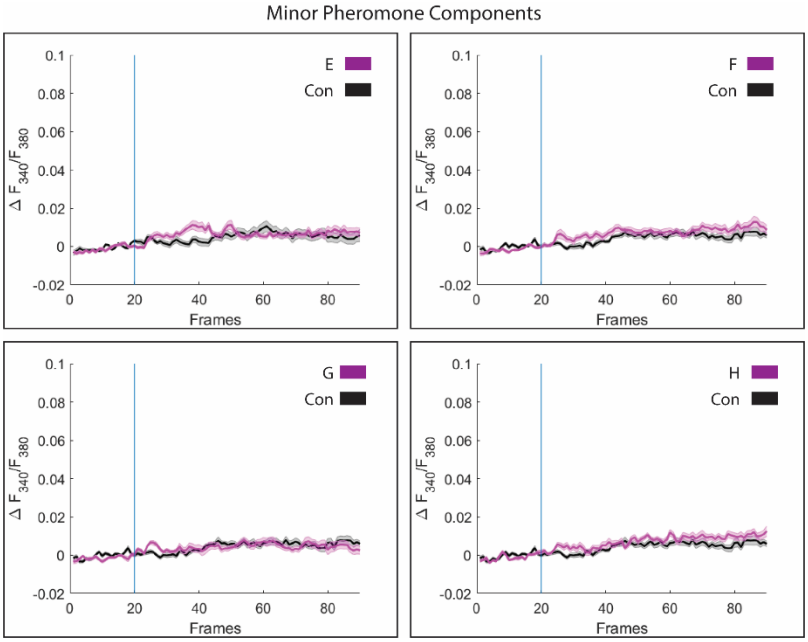

Figure 19. Mean + SE calcium traces of the PCx during stimulation with minor pheromone components E (14:Ald) (n=22), F (Z7-16:Ald) (n=22), G (9:Ald) (n=22), and H (7:Ald) (n=22). Each stimulus is presented twice. The blue vertical line represents the stimuli onset at frame 20

3.4 Comparison of odor-evoked responses to different stimulus concentrations

In order to obtain a suitable stimulus intensity for the calcium imaging, two different concentrations, 10^{-3} (20 µg) and 10^{-5} (200 ng), were used in the experiments. That gave us an opportunity to compare time traces for the same component at different concentrations. The traces presented in Figure 20-23 represent pure responses (control responses were subtracted from stimulus responses) of the three MGC units and the PCx to distinct concentration of the stimuli.

Regarding the cumulus, the primary pheromone component, A, elicited a response both when stimulating with 10^{-3} and 10^{-5}, however, the response patterns were somewhat different (Figure 20). The highest concentration elicited a stronger transient response, while the lower concentration elicited a weaker and more long-lasting response. The secondary pheromone component, B, and the interspecific component, C, also activated the cumulus when stimulating with the lower concentration, however, the higher concentration of these stimuli, did not evoke any activity.

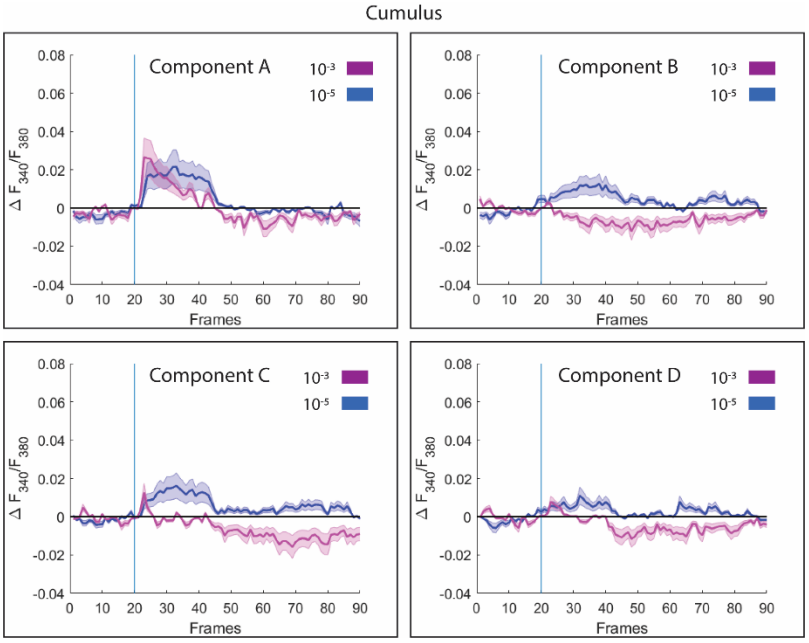

Figure 20. Show the mean ± SE Cumulus pure-responses to the two different concentration for component A-D. Traces for concentration 10^{-3} are from subject # 1-7, while the traces for 10^{-5} are from subject # 8-14. Each stimulus is presented twice. The blue vertical line represents the stimuli onset at frame 20.

As seen earlier, the DMA is particularly excited by the interspecific components, C and D. This holds true for both the high and low concentrations of the stimuli. Stimulation with the component C, however, revealed the same tendency as in the cumulus: the high concentration gives a strong transient response with a rapid decline in intracellular calcium levels, while the

lower concentration elicited a weaker response, which lasted throughout the stimulus period (Figure 21). In addition, the low concentration reached its peak response around frame 30-35, which is considerably later than what we observe for the higher concentration. For the interspecific component, D, however, the responses to the two concentrations seemed to last for approximately the same time, although, a transient peak in the trace for the higher concentration closely followed stimulus onset.

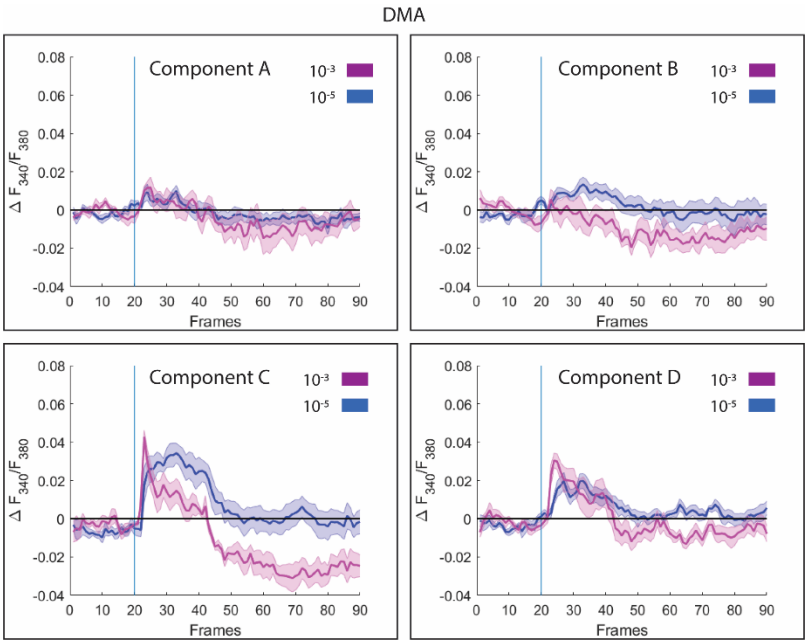

Figure 21. Show the mean ± SE DMA pure-responses to the two different concentration for component A-D. Traces for concentration 10^{-3} are from subject #1-7, while the traces for 10^{-5} are from subject #8-14. The blue vertical line represents the stimuli onset at frame 20

The secondary pheromone component, B, and the interspecific component, C, are responsible for the main excitation in the DMP (Figure 22). As seen in the DMA, the interspecific component C, also exhibits the same tendency in the DMP, where the higher concentration elicits a stronger activation with a rapid decline, while the lower concentration, elicit a weaker excitation that is better sustained throughout the stimulus period. The same tendency can be seen when stimulating with the secondary pheromone component B, however, for this component, the stronger concentration sustains a higher response throughout the stimulus period (Figure 22).

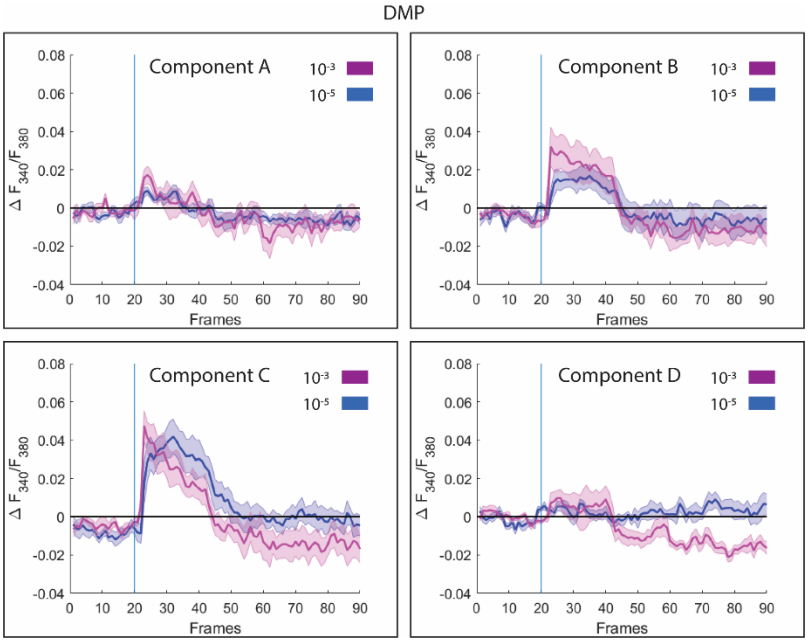

Figure 22. Show the mean ± SE DMP pure-responses to the two different concentration for component A-D. Traces for concentration 10^{-3} are from subject #1-7, while the traces for 10^{-5} are from subject #8-14. The blue vertical line represents the stimuli onset at frame 20.

In the PCx, the main response to one single component was induced by the interspecific component, C. Notably, the low concentration of stimulus C elicited a slightly higher response than the high concentration (Figure 23).

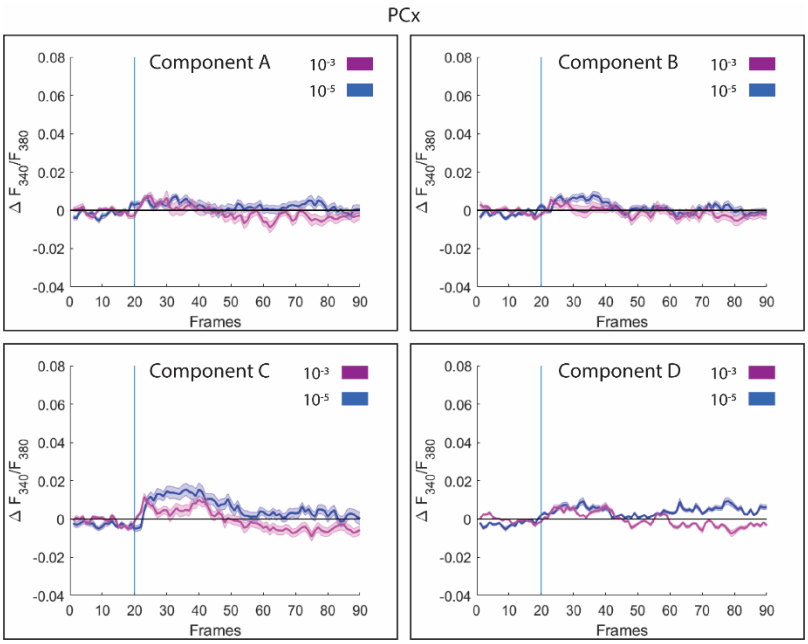

Figure 23. Show the mean ± SE PCx pure-responses to the two different concentration for component A-D. Traces for concentration 10-3 are from subject #1-7, while the traces for 10-5 are from subject #8-14. The blue vertical line represents the stimuli onset at frame 20.

4 Discussion

The present study demonstrates the first attempt to investigate the MGC and the PCx activity in a heliothine moth in response to a set of pheromone and interspecific components, using the current labeling technique. Here, I succeeded in labelling the medial-tract output neurons in several preparations. The application of odor stimuli onto the antenna of the living moth while performing calcium imaging, resulted in odor-specific responses in the labelled PNs, visualized as distinct activation maps of glomeruli in the MGC and PCx.

4.1 Functional characterization of the macro-glomerular complex

Each of the test components elicited its own distinct response pattern in the MGC when applied to the antenna. The cumulus was activated mainly by the primary pheromone component, A, the DMA mainly by the two interspecific components, C and D, and the DMP mainly by the secondary pheromone component, B, and the interspecific component, C. Overall, the three MGC glomeruli showed a fairly predictable response pattern when stimulated with different component blends. The general rule seems to be that if the blend contains a single component that elicited response in the given glomeruli, the blend evokes a response as well. The odor-induced activation patterns in each MGC glomerulus will be discussed in greater detail in the following section.

4.1.1 Odor-evoked responses in the cumulus

The results presented here show that all four stimuli evoking statistically significant responses in the cumulus included the primary pheromone component, A, making it the main driver of all responses in the cumulus. The results showing the primary pheromone component, A, as the only component eliciting response in the cumulus is in line with previous studies on *H. armigera* (Wu et al., 2015; Xu et al., 2016). However, both former investigations explored the *input* to the cumulus by combining electrophysiological recordings from the sensory neurons with bath application calcium imaging technique. The findings presented here, including information about the *output* from the cumulus, therefore indicate that the output is in correspondence with the input. Support for the assumption that the cumulus is a functional unit processing information about the primary pheromone component has been reported in several heliothine moth species (Christensen, Mustaparta, & Hildebrand, 1995; Vickers et al., 1998; Zhao & Berg, 2010).

It is also noteworthy that none of the blends containing the primary pheromone component, A, elicited a response significantly different from that of the single component A. In general, one might expect that the single component would elicit a stronger response, as the component blends have a lower amount of component A. For instance: if we use concentration 10^{-3} as an example, stimulating with component A alone, will correspond to a total amount of 20 µg of component A, while stimulating with the AB blend for instance will correspond to 10 µg of component A, yet, the blend and the single component elicits approximately the same response. This shows that not only is the primary pheromone component, A, the only component eliciting a response in the cumulus; but we can also conclude that no synergic effect can be seen when adding other components to its blend either. Also, this could indicate that the amount of each stimulus used both here and in other studies is unnecessary high, as lower amount of the same concentration elicits the same response.

4.1.2 Odor-evoked responses in the DMA

The fact that both interspecific signals, C and D, and the mixtures including these components, elicited significant responses in the DMA, indicates that this MGC-unit plays a special role in signaling the presence of a female from another species. Additionally, significant responses were elicited by component blends CD, and ABCD, and also, a weak but significant response can also be observed stimulating with the minor pheromone component, G. Smaller differences in the response can also be seen between the other four components (C, D, CD and ABCD); however, only component D and ABCD was significantly different form each other.

The responses in the DMA to component C and D are in full agreement with earlier studies using bath application (Wu et al., 2015; Xu et al., 2016). The significant difference in activity in the DMA when stimulating with the ABCD blend compared to component D alone can probably be explained by the fact that several of the OSNs innervating the DMA will be activated by the blend. Although, in *H. assulta* PNs sensitive to the interspecific component have reported inhibition of activity when stimulated with the primary pheromone component (Zhao & Berg, 2010); an effect that clearly cannot be observed here, as one should expect a decrease in activity when stimulating with the ABCD blend compared to the CD blend for instance. It should be noted that this response pattern was only shown in one of the PNs in the study mentioned above, whereas the majority of PNs probably do not show this characteristic; thus, when recording from the entire population, this response pattern of single PNs, is probably masked by the simpler response pattern of the majority of PNs.

4.1.3 Odor evoked responses in the DMP

The DMP exhibited a complex response pattern, including significant responses to six of the stimuli tested. Interestingly, the DMP was the only glomeruli that were activated when stimulating with the secondary pheromone component, B. This reflect the important role of the DMP in processing the secondary component which is connected with increased attraction of male *H. armigera*. Additionally, component A, C, AB, CD and ABCD elicited significant responses. The response to the primary pheromone component, A, however, was both transient and significantly weaker than all the other responses. It is also interesting that the activity patterns in the DMP when stimulating with the secondary pheromone component B, and the interspecific component C were distinctly different from each other.

Responses in the DMP to the secondary pheromone component, B, and the interspecific component, C, were expected based on electrophysiological data obtained from the male-specific sensilla trichodea in *H. armigera* (Wu et al., 2015; Xu et al., 2016). These previous data demonstrated that the sensory neurons tuned to the secondary pheromone, B, responded quite strongly to substance C as well. One might wonder what the reason for this is, as the interspecific component, C, has shown to decrease attraction in male *H. armigera,* having the opposite effect of the secondary pheromone component. This could be explained by the weak-shape theory, which suggest that the ORs in each OSN is exited strongly by one specific odor, and weaker to odors with a similar molecular shape (Jortner, 2013).

The response to the primary pheromone component, A, as shown in the present study, cannot be explained by physiological properties of the sensory neurons. The response to stimulus A was significantly weaker than the others, but anyway quite surprising. One possible explanation for this response, is that there are LN connections between the cumulus and DMP creating this excitation. Interestingly, previous data from intracellular recording/staining experiments in heliothine moths have found synergistic medial-tract neurons originating in the MGC-unit representing the second pheromone component (Berg et al., 1998; Vickers et al., 1998). Closely related heliothine species use many of the same pheromone components for sexual attractions (Baker, 2008; Kaissling, 1996). Therefore, this kind of 'blend-specific' neurons might play an essential role in ensuring high sensitivity to the species-specific ratio of the two behaviorally relevant pheromone constituents. In the results presented here, however, including stimulation both with the single pheromone components and the natural blend of these constituents as well as a 50/50 blend, demonstrated no synergistic effects. This indicates that the main portion of medial-tract neuron connected with DMP in *H. armigera* are not

'blend-neurons'. However, it is still possible that some of the individual DMP-PNs hold this physiological property.

4.2 Functional characterization of the posterior complex

Interestingly, the glomeruli included in the PCx, which were analyzed as one unit, exhibited a significant response to seven of the 12 tested stimuli, including the component blends ABn, CD, and ABCD, in addition to the four minor pheromone components, E-H. All these responses were, as expected, weak in comparison to those seen in the MGC (due to the clustering of the individual PCx glomeruli). In total, these results indicate that at least some of the glomeruli located in the PCx could be involved in pheromone processing. This is actually consistent with previous studies that have traced the male-specific OSNs in heliothine moths. Notably, sensory neurons tuned to Z11-16:AL (here named component A) are reported to be co-located with another sensory neuron in A-type sensilla in several species. While the heliothine moth neuron tuned to Z11-16:Al project to the MGC/cumulus, the co-located neuron targets one PCx glomerulus situated close to the MGC (Berg et al., 1998, 2005; Lee, Baker, et al., 2006; Lee, Carlsson, et al., 2006; Lee et al., 2016). Interestingly, the receptor for the neighboring neuron in the type A sensillum, named OR11, is identified in several of the above-mentioned heliothine species, *H. armigera* included, here named Harm11 (Chang et al., 2016). Additionally, in *H. subflexa* and *H. virescens* a neuron located in one of the type B sensilla trichodea has also been reported to project to another glomeruli located more dorsally in the PCx (Lee, Baker, et al., 2006; Lee et al., 2016).

Although the data presented here indicate that some of the glomeruli located in the PCx are involved in pheromone processing, it is unlikely that this is the main role of all ten glomeruli forming this complex. Interestingly, a subset of glomeruli located in the posterior part of the AL of the fruit fly, *Drosophila melanogaster*, has been shown to exclusively convey information regarding temperature and humidity (Enjin et al., 2016; Frank et al., 2017; Gallio, Ofstad, Macpherson, Wang, & Zuker, 2011; Liu, Mazor, & Wilson, 2015). These glomeruli however, are located more ventrally in the AL compared to the glomeruli confined to the PCx of the heliothine moths. Anyway, despite this slight difference in location, we should not exclude the possibility that some of these glomeruli could be analogs to those found in the fruit fly, conveying thermal information.

The calcium traces of the PCx responses showed some unusual response patterns, where the peak occurred relatively late in the stimulation period and not immediately after the stimulus onset. This indicates a substantial involvement of LNs in processing the odor signal before it is sent to the higher integration centers. Besides, an additional ''spike'' can be observed after the stimulus period which might be a result of inhibition release from LNs.

4.3 The effect of stimulating with different concentrations

In contrast to the quite unstable intracellular recording technique, calcium imaging offers the opportunity to measure neural activity during a longer time period. In this study, we included stimulation with different odor concentrations. In the MGC, stimulating with the two different concentrations of component A-D mainly created three different outcomes:

1) The glomeruli showed activity to more stimuli when stimulating with the lower concentration compared to the higher concentration. This can mainly be seen in cumulus, which has an excitation when stimulating with the lower concentration of stimuli B and C, which cannot be seen when stimulating with the high concentration. But can also be seen in the DMA when stimulating with the secondary pheromone component, B.

   A similar activity pattern has been found earlier in a calcium imaging study in *H. virescens,* where they also reported differences in activity of the MGC glomeruli when changing concentration of the very same component (Galizia, Sachse, & Mustaparta, 2000). In that study, the lower concentration (200 ng) lead to a strong activity in only one glomerulus, whereas the higher concentration (20 µg) induced weaker activation of two MGC glomeruli. It should be noted, though, that this study used the bath application method, which is assumed to primarily record the activity from the OSNs. The reason for this change in the activity pattern is unclear, although, one can assume that the LNs play a role here, having a stronger lateral inhibition from other glomeruli when a higher concentration is presented. If we use the secondary pheromone component, B, as an example. Using the stronger concentration, the secondary pheromone component only activates the DMP, however, using the lower concentration, smaller activity can also be seen in the

cumulus and DMA. This might be a result of the reduced LN activation in the DMA when stimulating with the lower concentration.

2) Another prominent trend that appears when comparing the responses to certain stimuli at different concentrations, is that the higher concentration elicits a strong and transient max response that peaks shortly after the stimulus onset. The lower concentration, on the other hand, elicits a smaller and less transient max response, that peaks close to the middle of the stimulus period. This response, however, is more stable and lasts throughout the stimulation period. This phenomenon can be observed in the cumulus, for example, when stimulating with the primary pheromone, A. Besides, it can be seen both the DMA and DMP during stimulation with the interspecific component, C.

   This change could probably also be explained by the involvement of the LNs playing a modulatory role; in this case, suppressing the stronger input and enhancing the weaker input from the OSNs. This difference in the temporal response pattern created by this modulation, is probably important for conveying information about different odor concentrations to the higher brain areas.
3) In other cases, the higher concentration just elicits an overall stronger response than the weaker concentration. This can be observed when stimulating with the interspecific component, D, in the DMA, and the secondary pheromone, B, in the DMP.

In the PCx on the other hand, both the high and low concentration of the interspecific component, C, evoked activity, however the excitation elicited by the lower concentration, seem to be overall stronger, this could possible also be an effect of the LNs as discussed above.

Earlier work has shown that the interspecific component, C, can function both as an interspecific component, reducing attraction, and a minor pheromone component, increasing attraction, when it is added to the pheromone blend (Gothilf, Kehat, Jacobson, & Galun, 1978; Kehat & Dunkelblum, 1990; Wu et al., 2015; Zhang et al., 2012). Summarized, this previous work indicates that component C increases attraction when 1% or less is added to the blend, whereas a higher concentration will reduce attraction. One could therefor expect that application of the low versus high concentration of component C might elicit responses in the DMP and DMA that somehow reflected the findings from the behavioral study. However,

stimulating with different concentrations of the interspecific component, C, did not induce an activity in the two MGC units reflecting the behavior reported above. The fact that this phenomenon can be seen in the behavioral studies, however, not when recording from the AL, indicate that this aspect of olfactory coding is not visible at the glomerular level, but rather is coded in higher brain areas of the olfactory pathway. It should be mentioned, that the investigations done here is somewhat different from those mentioned above, as they used component C in a mix together with the pheromone blend and we used the different concentrations of C as a single component.

4.4 The role of the minor pheromone components

The results presented here show that all the minor pheromone components elicited significant responses in the PCx; additionally, component G elicited a significant response in the DMA. However, all responses elicited by these minor components were weak, and they should therefore be tested more systematically. Several theories have been proposed on the function of the minor pheromone components. One hypothesized their role in increasing the attraction when added to the two principal pheromone components at correct concentrations (Baker, Cardé, & Roelofs, 1976; Bradshaw, Baker, & Lisk, 1983; Cardé, Baker, & Roelofs, 1975; Roelofs & Carde, 1977). Another theory implies that the minor components only contribute to the close-range interaction, being responsible for approach, landing, and courtship (Baker & Cardé, 1979; Linn, Campbell, & Roelofs, 1986, 1987). One of the newer theories suggests that the minor pheromone components not necessarily increase the attraction within the same species, but solely function as potential antagonists for related species, to help securing reproductive isolation (Mozūraitis & Būda, 2013). Recent research on the apple moth *Epiphyas postvittana* on the other hand, has indicated that the minor pheromone components do not necessarily increase the attraction when added to the blend with the primary pheromone component. However, adding the minor pheromone components to the blend when an interspecific component is also present, will reduce the effect of the interspecific component. Based on this research, it would be interesting to combine some of the minor pheromone components with the interspecific components, to investigate if such an interaction can be observed at the PN level in *H. armigera*.

4.5 Methodical considerations

4.5.1 Calcium imaging

Calcium imaging provides an excellent method of investigating the nervous system. In our case, the method grants us with the ability to measure odor-evoked responses in a distinct population of AL output neurons in live insects. This method can be used for an extended time period, allowing the usage of a relatively long list of stimuli, providing the possibility to accumulate high amounts of data for each preparation. Additionally, in our case the method works great in complimentary with the other method used in our lab: the intracellular recording and staining technique. Which makes it possible to measure the odor-evoked responses from the same PN category, from individual neurons using intracellular recording, and from the population, using calcium imaging. Although calcium imaging gives us a great opportunity to investigate neural systems, some inconveniences can be found to using this method. Doing in *vivo* imaging, there is no doubt that the preparation needs to be restrained properly to avoid movement, however, restraining the insect wasn't always enough, as in some preparation the movement was caused by the pumping of hemolymph through the head capsule area. No direct solution was found to this problem, however, during the processing of the data through KNIME, some of the movement was account for, although for preparations with too much movement, the program was unable to correct for it, and the data had to be discarded.

Another difficulty is trying to access various parts of the AL, as some parts are more hidden than others. This obstacle is encountered when trying to do calcium imaging of the PCx area in the AL. One is that it is hard to find the correct position for the preparation as you are not able to see what glomeruli you record from based on the raw data you have available; so, you do not know if the correct position was found before the data is processed through KNIME. To clarify, the PCx area is close to the protocerebrum, which means tilting it to much against a posterior view, will result in the protocerebrum covering the PCx, while tilting it to much against a frontal view will result in the MGC glomeruli covering the view. Some difficulties can also be found analyzing the data from the PCx, as part of the area also is close to the medial cell cluster which incorporates somata that also responded to some of the stimuli given. In some cases, where the AL map where somewhat obscured, the difference between a PCx glomerulus and a medial cell cluster somata where difficult to differentiate.

The calcium imaging is also dependent on which focal plane one decides to record from, being in the ‘’correct’’ focal plane is also hard to know before the data is processed, so again, it is based on an educated guess. Additionally, recording from the deeper focus plane is

difficult using this form of calcium imaging, as the imaging gets to blurry, meaning that only the superficial layer of the PCx glomeruli can be imaged.

4.5.2 Analysis

The decision of changing to a lower concentration during the project was based on the observation that some preparations displayed a global response including activation of many glomeruli when stimulating with the higher concentration (these preparations were excluded from the analysis). By changing to a lower concentration, the hope was to reduce this global response effect, by making the stimuli concentration more in line with what would occur in natural conditions. As high stimulus concentrations may activate a numerous type of sensilla trichodea, as the molecular structures of pheromones resemble each other (Hansson & Stensmyr, 2011). After changing to the lower concentration, the frequency of these global responses seemed to drop, however, it remains unclear if the global responses observed was due to the high concentration or some other reason.

The drawback of changing the concentration during the project however, where that extra thought had to be put into the analysis. For instance, to ensure a proper analysis of the data material, only a subset of the results was included in the statistical analysis to avoid any analytical source of error. By only using a subset of the data, we assured that the preparation included in the analysis had the same number of stimulations with each concentration. The negative aspect of doing this however is that all the results for the minor pheromone components and the other stimuli cannot be compared, as they contain subjects stimulated different concentrations. However, on the plus side, this allowed us to investigate the response differences to two different stimulus concentrations.

Another issue that is relevant to discuss is the definition of a response strength. Two main ways of specifying response strength come to mind. The one used here, was to define response strength according to the peak of the trace, demonstrating maximum fluorescence emission during the stimulation period. Alternatively, one could use an average value of the fluorescence emitted during this period. In some cases, the choice of definition might imply slightly different results; the clearest examples probably include the specification of response strength in DMP during application of stimulus A, and in the PCx during application of the minor pheromone components.

Although, the usage of different definition of response strength might give slight differences in the results, no optimal way of defining the response strength can be given when we are dealing with data having different temporal response patterns.

Throughout this project, different sample sizes are used for the different statistical testing. When doing significance testing of the effect of stimulating with the minor pheromone components in the MGC for instance, the sample size is 4-5 test subjects; for the other stimuli 7 subjects were used for significance testing in the MGC. While for the PCx the sample size was 22/23, since each ROI was treated as a test subject. These differences in the sample sizes will have an important effect on the p-value, as significance testing is highly dependent on the sample size. This means that the p-value is a result of both the effect studied and the sample size (Levine & Hullett, 2006). This in turn, means that there is a greater chance of finding a significant response in the PCx compared to the MGC. This effect however, could probably be look at as a compromise for pooling all the PCx glomeruli together, which results in an overall weaker effect of a stimulus. At the other end of the spectrum however, we have the stimulation with the minor pheromone components in the MGC which have a very small sample, the effect of a small sample in significance testing is an increased prevalence of type II errors, so important effects could be non-significant. When making the traces for the concentration differences, the sample size was also evaluated, and a choice to only include stimuli A-D was done, as these have the highest sample.

4.6 Further investigation

This project has demonstrated that selective labelling of the uniglomerular PNs is a suitable methodological approach for performing calcium-imaging measurements of odor-induced responses not only in the MGC of the moth brain, but also in the PCx. This methodological approach should be included in future investigations in order to obtain a deeper understanding of how the information is processed. Firstly, when it comes to the relatively well-described MGC, future studies might test more systematically the effect of distinct combinations of pheromone components, both as single components and blends. This might also contribute to a better insight into the modulatory role of the LN. Which in turn can help us understand the interplay between the glomeruli within either MGC or the PCx, and also between the inter-connected glomeruli belonging to these two anatomically different areas. Such an investigation could also clarify some of the questions discussed above, including: synergistic responses of

medial-tract PNs during stimulation with the two principal pheromone components, as found earlier, and the fact that the component blend including all components elicited as high or higher responses than the single components which have a higher total amount of the given compound.

Further studies should also probably use the lower concentration used in this study, as this concentration better reflects what is found in nature, and still proved reliable responses which also are adequate for imaging of the glomeruli activity. In order to study the effect of more complex blends, it would be interesting to test the minor pheromone components in combination with both the principal pheromones and the interspecific signals.

For the PCx, more information should be gathered by performing morphological and physiological characterizations of individual PNs innervating these glomeruli. Here, the method of intracellular recording and staining would be suitable. Pure morphological characterization could perhaps be combined with different types of mass staining as the PNs termination regions might tell us something about what kind of information is conveyed via this PN population, as pheromones and plant odors carried by medial-tract neurons have slightly different termination areas in the lateral protocerebrum (Homberg et al., 1988; Seki, Aonuma, & Kanzaki, 2005; Zhao et al., 2014). Tracing of individual PCx PNs could be done through targeting somata in the medial cell cluster, as these neurons have been reported to have their somata located there (Zhao, Chen, et al., 2016).

This study can give some insight into the functional significance of the previously unknown PCx and provide further studies with knowledge about potential stimuli which can be applied in future projects that aims to investigate this area.

5 Conclusion

1. Utilizing the method including retrograde staining of the uniglomerular PNs confined to the medial ALT exclusively made it possible to measure odor-elicited output responses from each of the three MGC-units and a collection of PCx glomeruli via calcium imaging.

2. The three identifiable MGC units displayed activation patterns during antennal stimulation with the female-produced components implying that two of the units (cumulus and DMP) are linked to attractive behavior whereas the third unit (DMA) is linked to inhibition of attraction.

- The largest MGC-unit, cumulus, displayed responses only during stimulation with component A or mixtures containing this constituent – indicating its special role in processing information about the primary pheromone component.
- The smaller MGC-unit located anteriorly, DMA, was activated during stimulation with the two interspecific signals and mixtures of these substances – indicating its role in processing interspecific-signal information.
- The smaller MGC-unit located posteriorly, DMP, was the only MGC-unit displaying significant responses during stimulation with component B – indicating its special role in processing information about the second pheromone component.
- The similar odor-evoked responses to single components and blends containing these constituents suggest that the responses from populations of medial-tract PNs occur mainly according to a labelled line principle.

3. The finding of statistically significant odor-responses in a collection of glomeruli included in the PCx, located dorsally in the AL, adjacent to the MGC, indicates that some of the PCx glomeruli are involved in processing information about pheromones and interspecific substances.

References

Ache, B. W., & Young, J. M. (2005). Olfaction: diverse species, conserved principles. *Neuron, 48*(3), 417-430. doi:10.1016/j.neuron.2005.10.022

Anton, S., & Homberg, U. (1999). Antennal Lobe Structure. In B. S. Hansson (Ed.). *Insect olfaction* (98-125). Berlin: Springer.

Baker, T. C. (2008). Balanced Olfactory Antagonism as a Concept for Understanding Evolutionary Shifts in Moth Sex Pheromone Blends. *Journal of Chemical Ecology, 34*(7), 971. doi:10.1007/s10886-008-9468-5

Baker, T. C., & Cardé, R. T. (1979). Analysis of Pheromone-Mediated Behaviors in Male Grapholitha molesta , the Oriental Fruit Moth (Lepidoptera: Tortricidae). *Environmental Entomology, 8*(5), 956-968. doi:10.1093/ee/8.5.956

Baker, T. C., Cardé, R. T., & Roelofs, W. L. (1976). Behavioral responses of male Argyrotaenia velutinana (Lepidoptera: Tortricidae) to components of its sex pheromone. *Journal of Chemical Ecology, 2*(3), 333-352. doi:10.1007/BF00988281

Baker, T. C., Ochieng', S. A., Cossé, A. A., Lee, S. G., Todd, J. L., Quero, C., & Vickers, N. J. (2004). A comparison of responses from olfactory receptor neurons of Heliothis subflexa and Heliothis virescens to components of their sex pheromone. *Journal of Comparative Physiology A, 190*(2), 155-165. doi:10.1007/s00359-003-0483-2

Berg, B. G., Almaas, T. J., Bjaalie, J. G., & Mustaparta, H. (1998). The macroglomerular complex of the antennal lobe in the tobacco budworm moth Heliothis virescens: specified subdivision in four compartments according to information about biologically significant compounds. *Journal of Comparative Physiology A, 183*(6), 669-682. doi:10.1007/s003590050290

Berg, B. G., Almaas, T. J., Bjaalie, J. G., & Mustaparta, H. (2005). Projections of male-specific receptor neurons in the antennal lobe of the Oriental tobacco budworm moth, Helicoverpa assulta: a unique glomerular organization among related species. *J Comp Neurol, 486*(3), 209-220. doi:10.1002/cne.20544

Berg, B. G., Schachtner, J., & Homberg, U. (2009). γ-Aminobutyric acid immunostaining in the antennal lobe of the moth Heliothis virescens and its colocalization with neuropeptides. *Cell and Tissue Research, 335*(3), 593-605. doi:10.1007/s00441-008-0744-z

Berg, B. G., Zhao, X. C., & Wang, G. (2014). Processing of Pheromone Information in Related Species of Heliothine Moths. *Insects, 5*(4), 742-761. doi:10.3390/insects5040742

Berridge, M. J., Lipp, P., & Bootman, M. D. (2000). The versatility and universality of calcium signalling. *Nature Reviews Molecular Cell Biology, 1*(1), 11-21. doi:10.1038/35036035

Bradshaw, J. W. S., Baker, R., & Lisk, J. C. (1983). Separate orientation and releaser components in a sex pheromone. *Nature, 304*(5923), 265-267. doi:10.1038/304265a0

Cardé, R. T., Baker, T. C., & Roelofs, W. L. (1975). Ethological function of components of a sex attractant system for oriental fruit moth males, Grapholitha molesta (Lepidoptera: Tortricidae). *Journal of Chemical Ecology, 1*(4), 475-491. doi:10.1007/BF00988588

Chang, H., Guo, M., Wang, B., Liu, Y., Dong, S., & Wang, G. (2016). Sensillar expression and responses of olfactory receptors reveal different peripheral coding in two Helicoverpa species using the same pheromone components. *Scientific Reports, 6*, 18742. doi:10.1038/srep18742

Chou, Y.-H., Spletter, M. L., Yaksi, E., Leong, J. C. S., Wilson, R. I., & Luo, L. (2010). Diversity and wiring variability of olfactory local interneurons in the Drosophila antennal lobe. *Nature Neuroscience, 13*, 439. doi:10.1038/nn.2489

Christensen, T. A., Mustaparta, H., & Hildebrand, J. G. (1995). Chemical communication in heliothine moths. *Journal of Comparative Physiology A, 177*(5), 545-557. doi:10.1007/BF00207184

Clyne, P. J., Warr, C. G., Freeman, M. R., Lessing, D., Kim, J., & Carlson, J. R. (1999). A novel family of divergent seven-transmembrane proteins: candidate odorant receptors in Drosophila. *Neuron, 22*(2), 327-338.

Cossé, A. A., Todd, J. L., & Baker, T. C. (1998). Neurons discovered in male Helicoverpa zea antennae that correlate with pheromone-mediated attraction and interspecific antagonism. *Journal of Comparative Physiology A, 182*(5), 585-594. doi:10.1007/s003590050205

Couto, A., Alenius, M., & Dickson, B. J. (2005). Molecular, Anatomical, and Functional Organization of the Drosophila Olfactory System. *Current Biology, 15*(17), 1535-1547. https://doi.org/10.1016/j.cub.2005.07.034

Dacks, A. M., Christensen, T. A., Agricola, H. J., Wollweber, L., & Hildebrand, J. G. (2005). Octopamine-immunoreactive neurons in the brain and subesophageal ganglion of the hawkmoth Manduca sexta. *J Comp Neurol, 488*(3), 255-268. doi:10.1002/cne.20556

Dacks, A. M., Christensen, T. A., & Hildebrand, J. G. (2006). Phylogeny of a serotonin-immunoreactive neuron in the primary olfactory center of the insect brain. *Journal of Comparative Neurology, 498*(6), 727-746. doi:10.1002/cne.21076

de Belle, J. S., & Heisenberg, M. (1994). Associative odor learning in Drosophila abolished by chemical ablation of mushroom bodies. *Science, 263*(5147), 692. doi:10.1126/science.8303280

Doty, R. L. (1986). Odor-guided behavior in mammals. *Experientia, 42*(3), 257-271.

Enjin, A., Zaharieva, E. E., Frank, D. D., Mansourian, S., Suh, G. S., Gallio, M., & Stensmyr, M. C. (2016). Humidity Sensing in Drosophila. *Curr Biol, 26*(10), 1352-1358. doi:10.1016/j.cub.2016.03.049

Frank, D. D., Enjin, A., Jouandet, G. C., Zaharieva, E. E., Para, A., Stensmyr, M. C., & Gallio, M. (2017). Early Integration of Temperature and Humidity Stimuli in the Drosophila Brain. *Curr Biol, 27*(15), 2381-2388. doi:10.1016/j.cub.2017.06.077

Galizia, C. G., Sachse, S., & Mustaparta, H. (2000). Calcium responses to pheromones and plant odours in the antennal lobe of the male and female moth Heliothis virescens. *J Comp Physiol A, 186*(11), 1049-1063.

Gallio, M., Ofstad, T. A., Macpherson, L. J., Wang, J. W., & Zuker, C. S. (2011). The coding of temperature in the Drosophila brain. *Cell, 144*(4), 614-624. doi:10.1016/j.cell.2011.01.028

Gao, Q., Yuan, B., & Chess, A. (2000). Convergent projections of Drosophila olfactory neurons to specific glomeruli in the antennal lobe. *Nature Neuroscience, 3*(8), 780-785. doi:10.1038/77680

Goldman, A. L., Van der Goes van Naters, W., Lessing, D., Warr, C. G., & Carlson, J. R. (2005). Coexpression of two functional odor receptors in one neuron. *Neuron, 45*(5), 661-666. doi:10.1016/j.neuron.2005.01.025

Gothilf, S., Kehat, M., Jacobson, M., & Galun, R. (1978). Sex attractants for male Heliothis armigera (Hbn.). *Experientia, 34*(7), 853-854. doi:10.1007/BF01939662

Grienberger, C., & Konnerth, A. (2012). Imaging Calcium in Neurons. *Neuron, 73*(5), 862-885. https://doi.org/10.1016/j.neuron.2012.02.011

Guerenstein, P. G., Christensen, T. A., & Hildebrand, J. G. (2004). Sensory processing of ambient CO2 information in the brain of the moth Manduca sexta. *Journal of Comparative Physiology A, 190*(9), 707-725. doi:10.1007/s00359-004-0529-0

Han, Q., Hansson, B. S., & Anton, S. (2005). Interactions of mechanical stimuli and sex pheromone information in antennal lobe neurons of a male moth, Spodoptera

littoralis. *Journal of Comparative Physiology A, 191*(6), 521-528. doi:10.1007/s00359-005-0618-8

Hansson, B. S. (1999). *Insect olfaction*. Berlin; London: Springer.

Hansson, B. S., Almaas, T. J., & Anton, S. (1995). Chemical communication in heliothine moths. *Journal of Comparative Physiology A, 177*(5), 535-543. doi:10.1007/BF00207183

Hansson, B. S., & Stensmyr, M. C. (2011). Evolution of insect olfaction. *Neuron, 72*(5), 698-711. doi:10.1016/j.neuron.2011.11.003

Heimbeck, G., Bugnon, V., Gendre, N., Keller, A., & Stocker, R. F. (2001). A central neural circuit for experience-independent olfactory and courtship behavior in Drosophila melanogaster. *Proceedings of the National Academy of Sciences, 98*(26), 15336-15341. doi:10.1073/pnas.011314898

Heisenberg, M., Borst, A., Wagner, S., & Byers, D. (1985). Drosophila Mushroom Body Mutants are Deficient in Olfactory Learning. *Journal of Neurogenetics, 2*(1), 1-30. doi:10.3109/01677068509100140

Hildebrand, J. G., & Shepherd, G. M. (1997). Mechanisms of olfactory discrimination: converging evidence for common principles across phyla. *Annu Rev Neurosci, 20*, 595-631. doi:10.1146/annurev.neuro.20.1.595

Hillier, N. K., & Baker, T. C. (2016). Pheromones of Heliothine Moths. In J. D. Allison & R. T. Cardé (Eds), *Pheromone communication in moths: evolution, behavior, and application* (301-333). Oakland: University of California Press

Homberg, U., Christensen, T. A., & Hildebrand, J. G. (1989). Structure and function of the deutocerebrum in insects. *Annu Rev Entomol, 34*, 477-501. doi:10.1146/annurev.en.34.010189.002401

Homberg, U., Montague, R. A., & Hildebrand, J. G. (1988). Anatomy of antenno-cerebral pathways in the brain of the sphinx moth Manduca sexta. *Cell Tissue Res, 254*(2), 255-281.

Hoskins, S. G., Homberg, U., Kingan, T. G., Christensen, T. A., & Hildebrand, J. G. (1986). Immunocytochemistry of GABA in the antennal lobes of the sphinx moth Manduca sexta. *Cell Tissue Res, 244*(2), 243-252.

Ian, E., Berg, A., Lillevoll, S. C., & Berg, B. G. (2016). Antennal-lobe tracts in the noctuid moth, Heliothis virescens: new anatomical findings. *Cell Tissue Res, 366*(1), 23-35. doi:10.1007/s00441-016-2448-0

Ian, E., Zhao, X. C., Lande, A., & Berg, B. G. (2016). Individual Neurons Confined to Distinct Antennal-Lobe Tracts in the Heliothine Moth: Morphological Characteristics and Global Projection Patterns. *Front Neuroanat, 10*, 101. doi:10.3389/fnana.2016.00101

Ito, K., Shinomiya, K., Ito, M., Armstrong, J. D., Boyan, G., Hartenstein, V., . . . Vosshall, Leslie B. (2014). A Systematic Nomenclature for the Insect Brain. *Neuron, 81*(4), 755-765. doi:https://doi.org/10.1016/j.neuron.2013.12.017

Jiang, X. J., Guo, H., Di, C., Yu, S., Zhu, L., Huang, L. Q., & Wang, C. Z. (2014). Sequence similarity and functional comparisons of pheromone receptor orthologs in two closely related Helicoverpa species. *Insect Biochem Mol Biol, 48*, 63-74. doi:10.1016/j.ibmb.2014.02.010

Jortner, R. A. (2013). Neural Coding in the Olfactory System. In R. Quian Quiroga & S. Panzeri (Eds.), *Principles of neural coding* (225-262). Boca Raton: Taylor & Francis.

Jortner, R. A., Farivar, S. S., & Laurent, G. (2007). A Simple Connectivity Scheme for Sparse Coding in an Olfactory System. *The Journal of Neuroscience, 27*(7), 1659-1669. doi:10.1523/JNEUROSCI.4171-06.2007

Kaissling, K.-E. (1996). Peripheral Mechanisms of Pheromone Reception in Moths. *Chemical Senses, 21*(2), 257-268. doi:10.1093/chemse/21.2.257

Karlson, P., & Lüscher, M. (1959). 'Pheromones': a New Term for a Class of Biologically Active Substances. *Nature, 183*(4653), 55. doi:10.1038/183055a0

Kaupp, U. B. (2010). Olfactory signalling in vertebrates and insects: differences and commonalities. *Nat Rev Neurosci, 11*(3), 188-200. doi:10.1038/nrn2789

Kehat, M., & Dunkelblum, E. (1990). Behavioral responses of maleHeliothis armigera (Lepidoptera: Noctuidae) moths in a flight tunnel to combinations of components identified from female sex pheromone glands. *Journal of Insect Behavior, 3*(1), 75-83. doi:10.1007/BF01049196

Keil, T. A. (1999). Morphology and Development of the Pheripheral Olfactory organs. In B. S. Hansson (Ed.). *Insect olfaction* (5-48). Berlin: Springer.

Kent, K. S., Harrow, I. D., Quartararo, P., & Hildebrand, J. G. (1986). An accessory olfactory pathway in Lepidoptera: the labial pit organ and its central projections in Manduca sexta and certain other sphinx moths and silk moths. *Cell and Tissue Research, 245*(2), 237-245. doi:10.1007/BF00213927

Kerr, J. N., Greenberg, D., & Helmchen, F. (2005). Imaging input and output of neocortical networks in vivo. *Proc Natl Acad Sci USA, 102*(39), 14063-14068. doi:10.1073/pnas.0506029102

Kido, A., & Ito, K. (2002). Mushroom bodies are not required for courtship behavior by normal and sexually mosaic Drosophila. *Journal of Neurobiology, 52*(4), 302-311. doi:10.1002/neu.10100

Laughlin, J. D., Ha, T. S., Jones, D. N. M., & Smith, D. P. (2008). Activation of Pheromone-Sensitive Neurons Is Mediated by Conformational Activation of Pheromone-Binding Protein. *Cell, 133*(7), 1255-1265. https://doi.org/10.1016/j.cell.2008.04.046

Laurent, G., & Naraghi, M. (1994). Odorant-induced oscillations in the mushroom bodies of the locust. *The Journal of Neuroscience, 14*(5), 2993. doi:10.1523/JNEUROSCI.14-05-02993.1994

Lee, S.-G., Baker, T. C., & Vickers, N. J. (2006). Glomerular Targets of Heliothis subflexa Male Olfactory Receptor Neurons Housed within Long Trichoid Sensilla. *Chemical Senses, 31*(9), 821-834. doi:10.1093/chemse/bjl025

Lee, S.-G., Carlsson, M. A., Hansson, B. S., Todd, J. L., & Baker, T. C. (2006). Antennal lobe projection destinations of Helicoverpa zea male olfactory receptor neurons responsive to heliothine sex pheromone components. *Journal of Comparative Physiology A, 192*(4), 351-363. doi:10.1007/s00359-005-0071-8

Lee, S. G., Poole, K., Linn, C. E., Jr., & Vickers, N. J. (2016). Transplant Antennae and Host Brain Interact to Shape Odor Perceptual Space in Male Moths. *PLoS One, 11*(1), e0147906. doi:10.1371/journal.pone.0147906

Lei, H., Christensen, T. A., & Hildebrand, J. G. (2002). Local inhibition modulates odor-evoked synchronization of glomerulus-specific output neurons. *Nature Neuroscience, 5*(6), 557-565. doi:10.1038/nn0602-859

Lei, H., Christensen, T. A., & Hildebrand, J. G. (2004). Spatial and Temporal Organization of Ensemble Representations for Different Odor Classes in the Moth Antennal Lobe. *The Journal of Neuroscience, 24*(49), 11108. doi:10.1523/JNEUROSCI.3677-04.2004

Levine, T. R., & Hullett, C. R. (2006). Eta Squared, Partial Eta Squared, and Misreporting of Effect Size in Communication Research. *Human Communication Research, 28*(4), 612-625. doi:10.1111/j.1468-2958.2002.tb00828.x

Linn, C. E., Campbell, M. G., & Roelofs, W. L. (1986). Male moth sensitivity to multicomponent pheromones: Critical role of female-released blend in determining

the functional role of components and active space of the pheromone. *Journal of Chemical Ecology, 12*(3), 659-668. doi:10.1007/BF01012100

Linn, C. E., Campbell, M. G., & Roelofs, W. L. (1987). Pheromone Components and Active Spaces: What Do Moths Smell and Where Do They Smell It? *Science, 237*(4815), 650. doi:10.1126/science.237.4815.650

Liu, L., Wolf, R., Ernst, R., & Heisenberg, M. (1999). Context generalization in Drosophila visual learning requires the mushroom bodies. *Nature, 400*(6746), 753-756. doi:10.1038/23456

Liu, W. W., Mazor, O., & Wilson, R. I. (2015). Thermosensory processing in the Drosophila brain. *Nature, 519*(7543), 353-357. doi:10.1038/nature14170

Liu, Y., Liu, C., Lin, K., & Wang, G. (2013). Functional specificity of sex pheromone receptors in the cotton bollworm Helicoverpa armigera. *PLoS One, 8*(4), e62094. doi:10.1371/journal.pone.0062094

Maleszka, J., Barron, A. B., Helliwell, P. G., & Maleszka, R. (2009). Effect of age, behaviour and social environment on honey bee brain plasticity. *Journal of Comparative Physiology A, 195*(8), 733-740. doi:10.1007/s00359-009-0449-0

Malun, D., Waldow, U., Kraus, D., & Boeckh, J. (1993). Connections between the deutocerebrum and the protocerebrum, and neuroanatomy of several classes of deutocerebral projection neurons in the brain of male Periplaneta americana. *J Comp Neurol, 329*(2), 143-162. doi:10.1002/cne.903290202

Martin, J. P., Beyerlein, A., Dacks, A. M., Reisenman, C. E., Riffell, J. A., Lei, H., & Hildebrand, J. G. (2011). The neurobiology of insect olfaction: sensory processing in a comparative context. *Prog Neurobiol, 95*(3), 427-447. doi:10.1016/j.pneurobio.2011.09.007

McBride, S. M. J., Giuliani, G., Choi, C., Krause, P., Correale, D., Watson, K., . . . Siwicki, K. K. (1999). Mushroom Body Ablation Impairs Short-Term Memory and Long-Term Memory of Courtship Conditioning in Drosophila melanogaster. *Neuron, 24*(4), 967-977. https://doi.org/10.1016/S0896-6273(00)81043-0

Menzel, R., Erber, J., & Masuhr, T. (1974). Learning and memory in the honeybee. In L. Barton-Browne (Ed.), *Experimental Analysis of Insect Behavior* (195-217). Berlin: Springer

Mizunami, M., Yokohari, F., & Takahata, M. (2004). Further exploration into the adaptive design of the arthropod "microbrain": I. Sensory and memory-processing systems. *Zoolog Sci, 21*(12), 1141-1151. doi:10.2108/zsj.21.1141

Mozūraitis, R., & Būda, V. (2013). Intra- and Interspecific Activities of Semiochemicals from the Sex Pheromone Gland of the Welsh Clearwing, Synanthedon Scoliaeformis. *Journal of Chemical Ecology, 39*(8), 1066-1069. doi:10.1007/s10886-013-0301-4

Roelofs, W. L., & Carde, R. T. (1977). Responses of Lepidoptera to Synthetic Sex Pheromone Chemicals and Their Analogues. *Annual Review of Entomology, 22*(1), 377-405. doi:10.1146/annurev.en.22.010177.002113

Rybak, J., Talarico, G., Ruiz, S., Arnold, C., Cantera, R., & Hansson, B. S. (2016). Synaptic circuitry of identified neurons in the antennal lobe of Drosophila melanogaster. *J Comp Neurol, 524*(9), 1920-1956. doi:10.1002/cne.23966

Rø, H., Muller, D., & Mustaparta, H. (2007). Anatomical organization of antennal lobe projection neurons in the moth Heliothis virescens. *J Comp Neurol, 500*(4), 658-675. doi:10.1002/cne.21194

Schachtner, J., Schmidt, M., & Homberg, U. (2005). Organization and evolutionary trends of primary olfactory brain centers in Tetraconata (Crustacea+Hexapoda). *Arthropod Structure & Development, 34*(3), 257-299. https://doi.org/10.1016/j.asd.2005.04.003

Seki, Y., Aonuma, H., & Kanzaki, R. (2005). Pheromone processing center in the protocerebrum of Bombyx mori revealed by nitric oxide-induced anti-cGMP immunocytochemistry. *Journal of Comparative Neurology, 481*(4), 340-351. doi:10.1002/cne.20392

Shang, Y., Claridge-Chang, A., Sjulson, L., Pypaert, M., & Miesenböck, G. (2007). Excitatory Local Circuits and Their Implications for Olfactory Processing in the Fly Antennal Lobe. *Cell, 128*(3), 601-612. https://doi.org/10.1016/j.cell.2006.12.034

Skiri, H. T., Rø, H., Berg, B. G., & Mustaparta, H. (2005). Consistent organization of glomeruli in the antennal lobes of related species of heliothine moths. *J Comp Neurol, 491*(4), 367-380. doi:10.1002/cne.20692

Steinbrecht, R. A. (1997). Pore structures in insect olfactory sensilla: A review of data and concepts. *International Journal of Insect Morphology and Embryology, 26*(3), 229-245. https://doi.org/10.1016/S0020-7322(97)00024-X

Stengl, M., Ziegelberger, G., Beoekhoff, I., & Krieger, J. (1999). Perireceptor Event and Transduction Mechanisms. In B. S. Hansson (Ed.), *Insect olfaction* (49-66). Berlin: Springer.

Stopfer, M. (2014). Central processing in the mushroom bodies. *Curr Opin Insect Sci, 6*, 99-103. doi:10.1016/j.cois.2014.10.009

Strauch, M., Rein, J., Lutz, C., & Galizia, C. G. (2013). Signal extraction from movies of honeybee brain activity: the ImageBee plugin for KNIME. *BMC Bioinformatics, 14*(18), S4. doi:10.1186/1471-2105-14-S18-S4

Sun, X. J., Tolbert, L. P., & Hildebrand, J. G. (1997). Synaptic organization of the uniglomerular projection neurons of the antennal lobe of the moth Manduca sexta: a laser scanning confocal and electron microscopic study. *J Comp Neurol, 379*(1), 2-20.

Tolbert, L. P., & Hildebrand, J. G. (1981). Organization and Synaptic Ultrastructure of Glomeruli in the Antennal Lobes of the Moth Manduca-Sexta - a Study Using Thin-Sections and Freeze-Fracture. *Proceedings of the Royal Society Series B-Biological Sciences, 213*(1192), 279-301. doi:DOI 10.1098/rspb.1981.0067

Tsien, R. Y. (1989). Fluorescent probes of cell signaling. *Annu Rev Neurosci, 12*, 227-253. doi:10.1146/annurev.ne.12.030189.001303

Vassar, R., Chao, S. K., Sitcheran, R., Nun˜ez, J. M., Vosshall, L. B., & Axel, R. (1994). Topographic organization of sensory projections to the olfactory bulb. *Cell, 79*(6), 981-991. https://doi.org/10.1016/0092-8674(94)90029-9

Vickers, N., Christensen, T., & Hildebrand, J. (1998). Combinatorial odor discrimination in the brain: Attractive and antagonist odor blends are represented in distinct combinations of uniquely identifiable glomeruli. *Journal of Comparative Neurology, 400*(1), 35-56.

Vosshall, L. B. (2000). Olfaction in Drosophila. *Curr Opin Neurobiol, 10*(4), 498-503.

Vosshall, L. B., Amrein, H., Morozov, P. S., Rzhetsky, A., & Axel, R. (1999). A spatial map of olfactory receptor expression in the Drosophila antenna. *Cell, 96*(5), 725-736.

Wu, H., Xu, M., Hou, C., Huang, L.-Q., Dong, J.-F., & Wang, C.-Z. (2015). Specific olfactory neurons and glomeruli are associated to differences in behavioral responses to pheromone components between two Helicoverpa species. *9*(206). doi:10.3389/fnbeh.2015.00206

Xu, M., Guo, H., Hou, C., Wu, H., Huang, L.-Q., & Wang, C.-Z. (2016). Olfactory perception and behavioral effects of sex pheromone gland components in Helicoverpa armigera and Helicoverpa assulta. *Scientific Reports, 6*, 22998. doi:10.1038/srep22998

Xu, W., Papanicolaou, A., Liu, N. Y., Dong, S. L., & Anderson, A. (2015). Chemosensory receptor genes in the Oriental tobacco budworm Helicoverpa assulta. *Insect Molecular Biology, 24*(2), 253-263. doi:10.1111/imb.12153

Zhang, J. P., Salcedo, C., Fang, Y. L., Zhang, R. J., & Zhang, Z. N. (2012). An overlooked component: (Z)-9-tetradecenal as a sex pheromone in Helicoverpa armigera. *J Insect Physiol, 58*(9), 1209-1216. doi:10.1016/j.jinsphys.2012.05.018

Zhao, X.-C., & Berg, B. G. (2010). Arrangement of Output Information from the 3 Macroglomerular Units in the Heliothine Moth Helicoverpa assulta: Morphological and Physiological Features of Male-Specific Projection Neurons. *Chemical Senses, 35*(6), 511-521. doi:10.1093/chemse/bjq043

Zhao, X.-C., Kvello, P., Løfaldli, B. B., Lillevoll, S. C., Mustaparta, H., & Berg, B. G. (2014). Representation of pheromones, interspecific signals, and plant odors in higher olfactory centers; mapping physiologically identified antennal-lobe projection neurons in the male heliothine moth. *8*(186). doi:10.3389/fnsys.2014.00186

Zhao, X.-C., Tang, Q.-B., Berg, B. G., Liu, Y., Wang, Y.-R., Yan, F.-M., & Wang, G.-R. (2013). Fine structure and primary sensory projections of sensilla located in the labial-palp pit organ of Helicoverpa armigera (Insecta). *Cell and Tissue Research, 353*(3), 399-408. doi:10.1007/s00441-013-1657-z

Zhao, X. C., Chen, Q. Y., Guo, P., Xie, G. Y., Tang, Q. B., Guo, X. R., & Berg, B. G. (2016). Glomerular identification in the antennal lobe of the male moth Helicoverpa armigera. *J Comp Neurol, 524*(15), 2993-3013. doi:10.1002/cne.24003

Zhao, X. C., Ma, B. W., Berg, B. G., Xie, G. Y., Tang, Q. B., & Guo, X. R. (2016). A global-wide search for sexual dimorphism of glomeruli in the antennal lobe of female and male Helicoverpa armigera. *Sci Rep, 6*, 35204. doi:10.1038/srep35204

Appendix A

Results of all t-test comparing stimuli responses to the control response

Appendix Table 1.Results of all t-test comparing stimuli responses to the control response, in the cumulus and the DMA. n, number of subjects; SD, standard deviation; t, t-value; df, degrees of freedom.

Cumulus						
Stimulus	n	Mean	SD	t(df)	p	Cohen's d_z
Control	7	0.025	0.013			
A	7	0.045	0.018	5.516(6)	0.001	2.085
B	7	0.023	0.016	0.423(6)	0.687	-0.160
C	7	0.027	0.011	0.801(6)	0.454	0.303
D	7	0.029	0.015	1.330(6)	0.232	0.503
AB	7	0.044	0.019	4.522(6)	0.004	1.709
ABn	7	0.042	0.012	4.059(6)	0.007	1.534
CD	7	0.029	0.017	1.434(6)	0.202	0.542
ABCD	7	0.049	0.018	5.366(6)	0.002	2.028
Cumulus – Minor Pheromone Components						
Hexane Con.	4	0.014	0.014			
E	4	0.008	0.007	-0.928(3)	0.422	0.464
Control	4	0.002	0.005			
F	4	0.006	0.003	1.066(3)	0.365	0.533
G	4	0.012	0.008	1.506(3)	0.229	0.753
H	4	0.008	0.004	1.619(3)	0.204	0.810
DMA						
Stimulus	n	Mean	SD	t(df)	p	Cohen's d_z
Control	7	0.031	0.016			
A	7	0.040	0.023	1.727(6)	0.135	0.653
B	7	0.037	0.027	0.849(6)	0.428	0.321
C	7	0.059	0.014	8.979(6)	<0.001	3.394
D	7	0.053	0.020	7.785(6)	<0.001	2.942
AB	7	0.039	0.023	1.468(6)	0.192	0.555
ABn	7	0.039	0.014	2.192(6)	0.071	0.829
CD	7	0.061	0.025	4.425(6)	0.004	1.672
ABCD	7	0.066	0.023	6.771(6)	<0.001	2.559
DMA – Minor Pheromone Components						
Hexane Con.	5	0.011	0.008			
E	5	0.011	0.007	-0.070(4)	0.947	0.032
Control	5	0.007	0.006			
F	5	0.012	0.009	0.999(4)	0.374	0.447
G	5	0.014	0.005	3.110(4)	0.036	1.391
H	5	0.011	0.005	1.566(4)	0.192	0.700

Appendix Table 2. Results of all t-test comparing stimuli responses to the control response, in the DMP and the PCx. n, number of subjects; SD, standard deviation; t, t-value; df, degrees of freedom.

DMP						
Stimulus	Nr.	Mean	SD	t(df)	p	Cohen's d_z
Control	7	0.022	0.013			
A	7	0.035	0.017	3.189(6)	0.019	1.205
B	7	0.053	0.029	3.702(6)	0.010	1.399
C	7	0.64	0.028	4.590(6)	0.004	1.735
D	7	0.024	0.010	0.602(6)	0.569	0.228
AB	7	0.042	0.020	3.481(6)	0.013	1.316
ABn	7	0.029	0.014	1.990(6)	0.094	0.752
CD	7	0.060	0.028	4.119(6)	0.006	1.557
ABCD	7	0.065	0.032	4.776(6)	0.003	1.805
DMP – Minor Pheromone Components						
Hexane Con.	5	0.011	0.009			
E	5	0.016	0.015	0.964(4)	0.390	0.431
Control	5	0.009	0.007			
F	5	0.017	0.016	0.958(4)	0.392	0.429
G	5	0.014	0.008	0.993(4)	0.377	0.444
H	5	0.013	0.007	2.352(4)	0.078	1.052
PCx						
Stimulus	Nr.	Mean	SD	t(df)	p	Cohen's d_z
Control	23	0.020	0.014			
A	23	0.024	0.010	1.166(22)	0.256	0.243
B	23	0.022	0.012	0.661(22)	0.515	0.138
C	23	0.025	0.009	1.764(22)	0.092	0.368
D	23	0.024	0.013	1.499(22)	0.148	0.313
AB	23	0.020	0.009	0.035(22)	0.972	0.007
ABn	23	0.027	0.011	2.719(22)	0.013	0.567
CD	23	0.026	0.013	2.078(22)	0.050	0.433
ABCD	23	0.031	0.014	3.956(22)	<0.001	0.825
PCx – Minor Pheromone Components						
Hexane Con.	22	0.009	0.007			
E	22	0.015	0.009	3.552(21)	0.002	0.757
Control	22	0.008	0.003			
F	22	0.012	0.007	2.483(21)	0.022	0.529
G	22	0.012	0.007	2.671(21)	0.014	0.570
H	22	0.011	0.004	4.174(21)	<0.001	0.890